Chapter IV

The immune response of *Anopheles* to malaria

1 The understated importance of the mosquito immune system in developing effective transmission-blocking strategies for malaria

"It's time to close the books on infectious diseases, and declare war against pestilence won"

When dealing with vector-transmitted infectious diseases, the importance of the vector's immune system has long been underappreciated. Only in the last few years has interest in so-called transmission blocking strategies (TBS) blossomed. These are different from traditional control measures in that they do not kill mosquitoes, and do not select them towards survival like insecticides [15, 358]. Three main strategies are being evaluated. The first entails killing gametocytes with drugs to stop mosquito midguts colonisation. The second pursues the same goal by vaccinating a population against the late human or early mosquito life stages of malaria. And the last seeks to make the mosquitoes refractory to infection and transmission. Especially for the latter, a thorough understanding of how the immune system of mosquitoes works both with blood-feeding and with immune challenge is required. Mosquitoes do not possess an adaptive immune response and as such rely solely on innate defence mechanisms. As such, the malaria parasite did not need to develop immune-evasion strategies quite as sophisticated in mosquitoes than in humans. And that represents an opportunity for intervention.

Three main strategies have been employed to increase the number of malaria-refractory mosquitoes: replacement of the native mosquito population, artificial gene drive, and use of other organisms for delivery. In all cases effective anti-malarial molecules are required. Phospholipase A2 (PLA2) has already been trialled as one such effector molecule [359]. While the mechanism was originally unknown, work in our laboratory (see main introduction) demonstrated the importance of eicosanoids (LXA_4 and PGE_2) in controlling malaria infection. As the upstream enzyme in the eicosanoid pathway, PLA2 at least partially decreases oocysts load by increasing the availability of eicosanoids in the mosquito. Another molecules used to control infection has been the gland and midgut peptide 1 (SM1), which blocks recognition sites of sporozoites and ookinetes [360].

The immune response of *Anopheles gambiae* to malaria

The most potent molecule is still useless without efficient delivery systems, or an effective way to release modified mosquitoes in the wild. Population replacement is the simplest approach, but requires initial native mosquito elimination campaigns to decrease the number of local susceptible mosquitoes. Furthermore, even the slightest fitness cost will result in the need for continuous releases of modified organisms. Not to mention the important ethical issues related to releasing biting *Anopheles* mosquitoes around human populations. An alternative is the use of gene drive systems, which can decrease the amounts of mosquito releases required, and thus spread malaria resistance faster and more effectively (or even eliminate malaria-transmitting species altogether) [361]. Finally, bacteria and fungi can also be harvested as expression systems for *Plasmodium*-killing molecules, as was done with a strain of *Escherichia coli* expressing a fusion antibody against Pbs2, thereby reducing oocyst load by 95% [362]. Another example is a fusion protein of SM1 and scorpine (antimicrobial toxin) in the fungus *Metarhizium anisopliae*. These fungal spores were able to decrease *P. falciparum* sporozoites by 98% in *A. gambiae*. Alternatively, the bacterium *Wolbachia* has shown direct transmission-blocking effects, but there are limitations in terms of natural *Wolbachia* density levels [363].

All in all, the number of effector molecules and delivery strategies that could induce a refractory state in mosquitoes remain limited, and more research is required into the way *Plasmodium* colonises *Anopheles,* and how the mosquito's immune system responds to infection. A thorough understanding of the immune system of mosquitoes is crucial to stop transmission of diseases such as malaria that are spread by arthropod vectors. The mosquito's immune system limits *Plasmodium* infection in several ways[364, 365], and hemocytes, the insect white blood cells, are key players in these defense responses[366, 367]. Ookinete invasion triggers a strong nitration response in invaded midgut epithelial cells and their basal lamina[368, 369]. Hemocytes that come in contact with a nitrated midgut basal lamina release microvesicles into the epithelial basal labyrinth and promote local complement activation, inducing parasite lysis[367]. An infection with *Plasmodium* primes mosquitoes to mount a stronger immune response to subsequent infections[370]. Primed mosquitoes release a

hemocyte differentiation factor (HDF) into the hemolymph[370], consisting of a complex of lipoxin A4 bound to the lipocalin carrier evoking [371]. HDF increases the proportion of circulating granulocytes, promotes microvesicle release, and enhances complement-mediated parasite lysis[367]. Enhanced immunity is lost if HDF synthesis is blocked[371]. Silencing the transcription factor LL3 also disrupts priming, and LL3 is expressed in hemocytes[372]. However, it is not clear whether LL3 is essential for HDF synthesis or for hemocytes to respond to HDF, nor which hemocyte subtypes express LL3.

In this chapter we shed light on the role of LL3 and of a subset of hemocytes (effector cells) in orchestrating the hemocyte responses to HDF. We also explored how the cell populations we identified in Chapter III change with blood feeding and infection, and we looked at whether the increase in circulating granulocytes is solely due to granulocyte proliferation and differentiation from prohemocytes or also to mobilization of sessile hemocytes. And finally, we assessed the transcriptomic changes brought about by blood feeding and *P. berghei* infection via both scRNA-seq and bulk RNAseq.

The immune response of *Anopheles gambiae* to malaria

1.1 Aims

1. To explore how the immune system of *Anopheles* mosquitos reacts to blood feeding and *P. berghei* or *P. falciparum* infection.
2. To determine cell types and states associated with malaria infection
3. To explore the role of LL3 in priming
4. To identify genes associated with immunity to malaria and anti-plasmodial effector states
5. To visualise how hemocyte populations change in time and space after *P. berghei* or *P. falciparum* infection, both on the surface of the body wall and the gut, and in circulation.

1.2 Colleagues

Dr. Ana Beatriz Barletta-Ferreira and the NIH imaging core prepared and imaged the isolated P. *berghei*-infected hemocyte RNA-FISH. Alvaro Molina Cruz and Gaspar Canepa grew the *P. falciparum* cultures. Rafael Cantera took care of the electron-microscopy. Jose Luis Ramirez performed the LL3 experiment. All other data and analyses presented is a result of my own work unless stated otherwise.

2 Methods

Most experiments in this thesis were performed in my other laboratory at the National Institutes of Health (NIH), and as such employed A. gambiae (G3 NIH strain) rather than the A. gambiae M-form (A. coluzzi) used for the scRNA-seq experiments.

2.1 *A. gambiae* mosquito rearing and *P. falciparum* infection

A. gambiae (G3 NIH strain) and *A. gambiae* M-form (*A. coluzzi*) were reared at 28 °C, 80% humidity, 12-hour light/dark cycle with standard laboratory procedures. The *P. falciparum* strains used were NF54 (WT *P. falciparum*), and NF54-Pfs47KO (Knock-out *P. falciparum*). They were maintained in O^+ human erythrocytes with RPMI 1640 medium with 25 mM HEPES, 50 mg/l hypoxanthine, 25 mM $NaHCO_3$, and 10% (v/v) heat-inactivated type O^+ human serum supplementation (Interstate Blood Bank, Inc., Memphis, TN) at 37°C and with a gas mixture of 5% O_2, 5% CO_2, and balance N_2. *P. falciparum* infections were done by diluting to 0.1% gametocytemia mature NF54 gametocytes. Mosquitoes were then allowed to feed with an artificial membrane feeder. NF54 with human red blood cells to 45% haematocrit was placed in warmed to 37C water-jacketed glass membrane feeders and mosquitoes allowed to feed for 20 minutes. Fed mosquitoes were then incubated at 26°C and 80% humidity. Infection levels (oocyst numbers) were checked by first dissecting midguts in 1× PBS and then staining them in 0.1% mercurochrome ahead of compound microscope visualization.

2.2 *A. gambiae* dsRNA micro-injections and LL3 knockdown

Two to three-day old female *A. gambiae* G3 mosquitoes were cold anesthetized and injected with 69 nl of 3 μg/μl dsRNA solution specific for LacZ, a bacterial gene not found in the genome of mosquitoes. dsRNA of LacZ is used as control during dsRNA-injection gene knockdown. A 218-bp fragment was amplified from LacZ gene cloned into pCRII-TOPO vector using M13 primers to add a T7 tail. For dsLL3 synthesis, a fragment was amplified with a T7 tail using the following primers as previously described:

T7-LL3 F -
TTAATACGACTCACTATAGGGAGAATGACTACCATCATAGTGACGAACCC
T7-LL3 R –
TTAATACGACTCACTATAGGGAGATTACACCATTATTAAATAAATAACACAACTT
GAG.
The PCR product, from LacZ and LL3, was used as a template for dsRNA synthesis with Megascript RNAi kit (ThermoFisher Scientific) according to the manufacturer's instructions.

2.3 Generation of naïve (-HDF) and challenged (+HDF) hemolymph and injection in LL3-knockdown recipients

Mosquitoes were infected with *P. berghei* and following blood feeding, the naive group was placed at 28^{o}C to prevent infection; while the challenged group was maintained at 21^{o}C for 48h, for normal infection to proceed. Subsequently, the challenged group was transferred to 28^{o}C to reduce parasite load. Hemolymph from naïve and challenged groups was collected at seven days post-infection and centrifuged at 4^{o}C, 10,000 rpms for 10 min. The cell-free supernatant was transferred to a new microcentrifuge tube and stored at -80^{o}C until its use. To evaluate the effects of LL3 depletion on the hemocyte's capacity to respond to HDF, 2-3-day old mosquitoes injected with dsRNA for LL3 or LacZ (control) were then injected with 138 nl of cell-free hemolymph from Naïve (- HDF) or Challenged (+ HDF) donors at 3 days post-silencing. Hemocyte differentiation was assessed in two independent experiments at four days post-hemolymph transfer.

2.4 Imaging

RNA-FISH performed as of Chapter II and III. EM performed by Dr. Rafael Cantera.

2.4.1 Image analysis

Acquisition as of Chapter III. For image analysis see below. Whole-mount RNA-FISH positive cells were manually counted by an observer blinded to experimental conditions using the

3DHISTECH CaseViewer 2.3 software (3DHISTECH, Budapest, Hungary). Body wall and gut areas were measured with the analysis tools of the same software. For *P. falciparum* RNA-FISH experiments of hemocytes in circulation, positive cells were counted automatically using the segmentation and thresholding features of the Leica LAS X 3D visualization and analysis software (Leica UK, Milton Keys, UK). For *P. berghei* RNA-FISH experiments of hemocytes in circulation, image processing was performed using Imaris 9.2.1 (Bitplane, Concord, MA, USA). Error bars represent 95% confidence intervals calculated with the T-test distribution on the number of samples obtained, and the standard deviation of the samples for each condition.

2.5 Bioinformatics

2.5.1 Bulk RNA-seq

Sequencing reads in CRAM format were fed into a personal BASH pipeline to convert cram files to fastq using biobam's bamtofastq program (Version 0.0.191). Forward and reverse fastq reads in paired mode were aligned to the *A. gambiae* AgamP4.3 reference genome using hisat2 (Version 2.0.4) and featureCounts (Version 1.5.1) with recommended settings. Count matrices were combined before downstream data processing and analysis within R version 3.5.3 (RStudio version 1.0.153). Downstream normalization, differential expression analysis and visualization were done with the R package DESeq2 (Version 1.18.1) [280], as of chapter III. P values for the differential expression analysis were adjusted for multiple testing using the Bonferroni correction. Genes were considered as differentially expressed if they had an adjusted P value < 0.001 (Wald T-test) and a $\log_2$ fold change > 2. Gene lists with vectorbase IDs were converted to gene annotations with g:Profiler [346]. g:Profiler utilises Ensembl as its primary data source and is anchored to its quarterly release cycle. g:GOSt was used to perform functional enrichment analysis on input gene lists to map the data onto enriched biological processes or pathways. In addition to Ensembl, also KEGG, Reactome, WikiPathways, miRTarBase, and TRANSFAC databases were used. Functional enrichment is evaluated with a cumulative hypergeometric test with g:SCS (Set Counts and Sizes) multiple testing correction (adjusted P value reported only < 0.05). Gene lists were ordered on log-fold changes. Each body part DE analysis was run separately, removing samples from all other body parts from

the matrices. The following model was then run for differential expression analysis, focused on treatment (*P. berghei* vs blood fed, and blood fed vs sugar fed). Experimental repeats, time, and effect of treatment at different time-point were considered as covariates:

```
ddsMat <- DESeqDataSetFromMatrix(countData = countdata, colData = coldata, design
= ~ time:treatment + experiment + time + treatment)
```

2.5.2 scRNA-seq

For details see methods Chapter II and III. For cell number normalization cells were first normalised to 10,000 total cells across all cell states in each condition. The percentage of cells in each cluster by condition was then calculated on the total normalised cells per cluster. Specific differential expression analyses were performed using the R package Seurat 3.0.2) [256, 277, 339]. Batches were integrated with a hybrid CCA / MNN strategy identifying 'anchors': cells with similar transcriptomes between conditions. Analysis of differentially expressed genes to identify marker genes for each cell population was performed based on the Wilcoxon rank-sum test (minimum Log Fold Change > 0.25, maximum adjusted P value 0.05). P values were adjusted for multiple testing using the Bonferroni correction. Differential expression analysis between sugar feeding, blood feeding, and *P. berghei* infection was performed with both Wilcoxon rank-sum test (minimum Log Fold Change > 0.25, maximum adjusted P value 0.05) and with a MAST (Model-based Analysis of Single-cell Transcriptomics) package adaptation for Seurat [279]. MAST is a differential expression analysis tool specifically developed for single-cell datasets, which employs a generalized linear model framework that considers cellular detection rate of genes as a covariate in the model. Volcano plots and labels were plotted with the Enhanced Volcano Plot package for R [373]. Gene lists containing vectorbase transcript IDs were converted to usable gene annotations, GO terms, and GO enrichment lists using g:Profiler for *A. gambiae* [346].

3 Results

3.1 Cell populations change with blood feeding and malaria infection

To explore how our immune populations change with infection and blood-feeding we first quantified the proportion of cells – as defined in our scRNAseq experiment – in each cell state by treatment. We found that samples infected with *P. berghei* showed an increased number of active type 1 and type 2 granulocytes. On the other hand, *P. berghei* treatment decreased the proportion of cells categorized as baseline granulocytes. Dividing cells and effector cells increased almost equally with both blood fed and infection, whereas secretory cells increased mostly with blood-feeding. Furthermore, oenocytoids increased with both blood feeding and *P. berghei* infection, whereas prohemocytes decreased. With regards to non-hemocytes, there was a higher number of baseline fat body cells with sugar feeding, whereas activated fat body appear to be enriched after *P. berghei* infection.

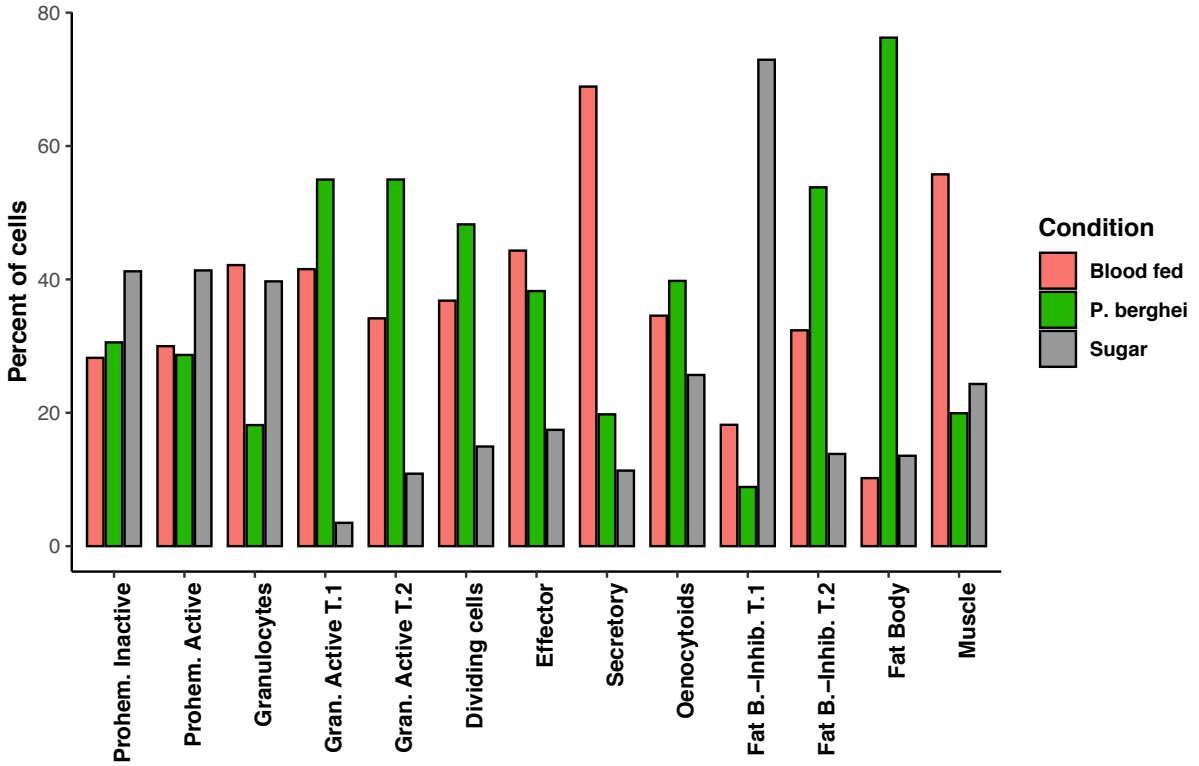

Fig. IV.1 Percentage of cells in each cluster by condition. Cell numbers first normalised to 10,000 total cells across all cell states in each condition. Then the percentage of cells in each cluster by condition was calculated on the total normalised cells per cluster.

Similarly, when we removed all cells that were not hemocytes from the calculations and again normalized the contribution of each cell state to the total number of remaining cells for each condition, we saw the same pattern, suggesting non-hemocytes were not skewing the calculations. The marked decrease in prohemocytes and correspondent increase in granulocytes appeared even more evident. The increased number of active granulocytes with malaria infection as compared to blood feeding or sugar feeding was also clearer. Conversely, secretory cells increased with blood feeding.

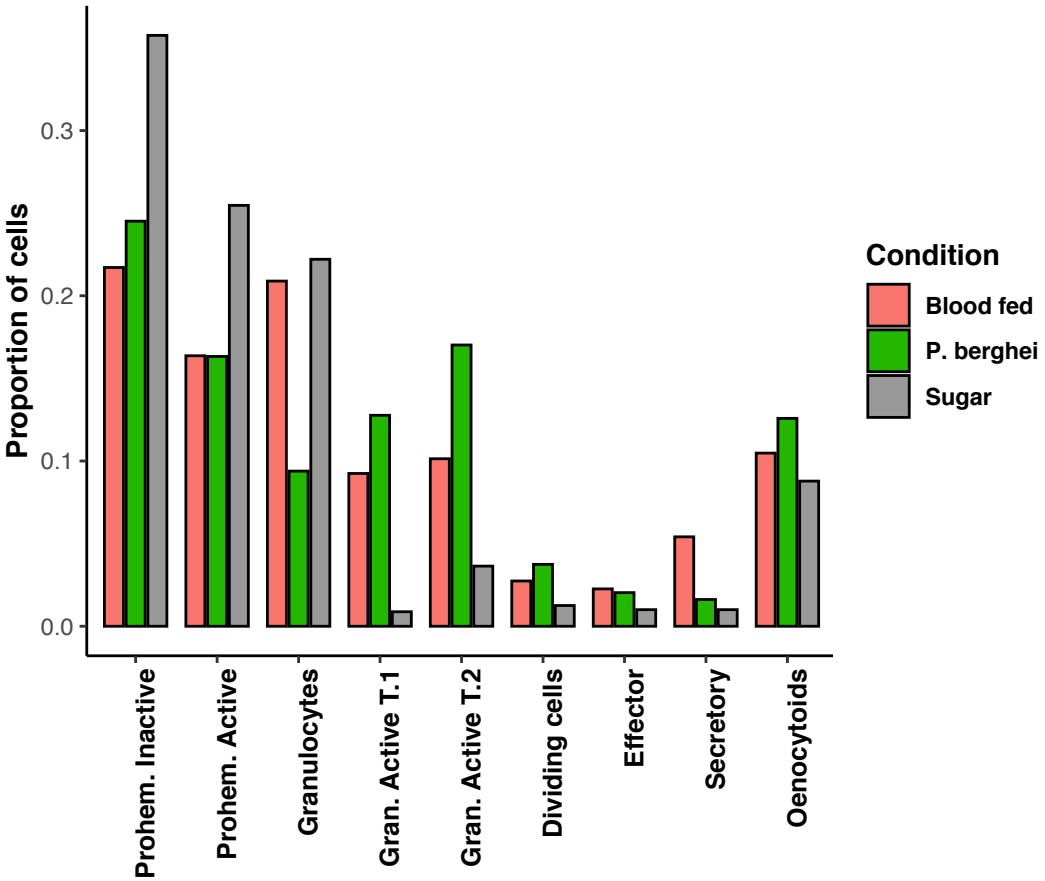

Fig. IV.2 Proportion of cells in each condition by cluster. Cell numbers first normalised to the percentage of cells in each condition that are hemocytes. Then the proportion by which each cluster contributed to the total number of remaining cells in each condition was recalculated.

Importantly, total cell numbers could be directly compared with manual hemocyte counts. The proportion of prohemocytes were 70.9% with blood feeding and 71.5% with *P. berghei* infection. Oenocytoids went from 23.2% with blood feeding to 17% with *P. berghei*. Granulocytes changed from 5.9% with blood feeding to 11.5% with *P. berghei* infection, which was statistically significant (P = 0.0073). The numbers from the manual hemocyte counting and single-cell RNAseq were largely in agreement. Prohemocyte counts were higher with manual counting, further suggesting a degree of similarity between prohemocytes and granulocytes. *P. berghei* infected mosquitoes were checked for infection [Fig. IV.3], and all mosquitoes were infected, with a median of 10 oocysts per midgut.

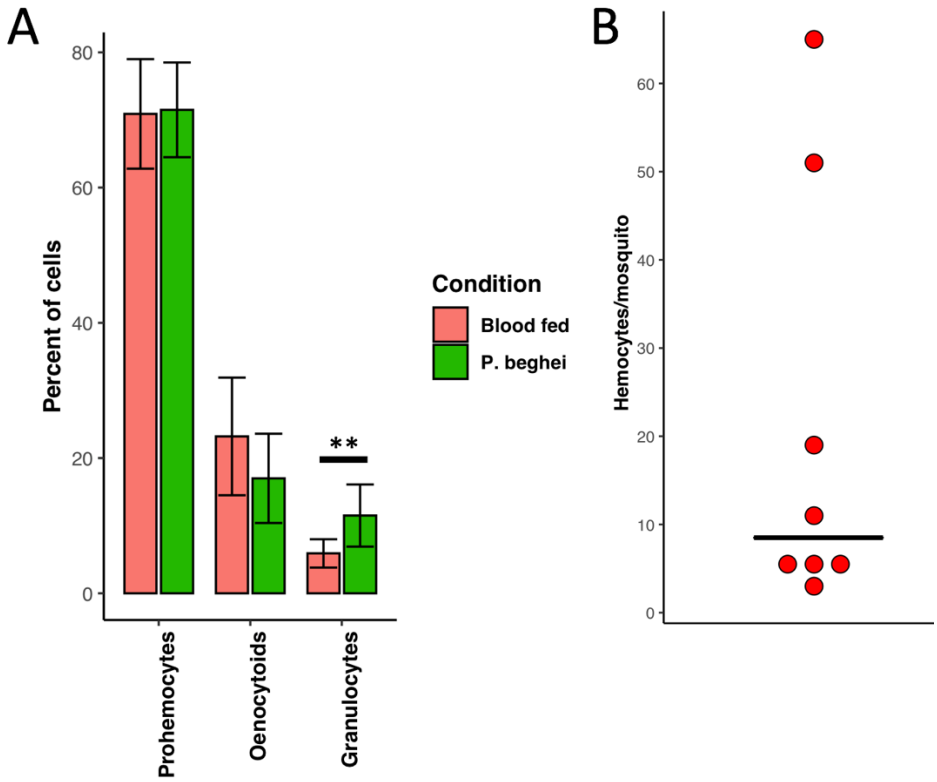

Fig. IV.3 Manual counting of hemocytes and oocysts. (A) 8 mosquitoes were dissected and hemocytes counted with hemocytometer. (B) 8 mosquitoes from the same experiment were dissected and oocysts checked with fluorescence microscopy for oocysts of GFP-CON *P. berghei*. Two repeats. Error bars are mean +/- standard deviation for the population for each sample. ** (P = 0.0073)

3.2 Transcription factor LL3 is required for hemocyte differentiation during immune priming

We have mentioned how the transcription factor LL3 can be detected in granulocytes from *Plasmodium*-infected *A. gambiae,* and that silencing LL3 expression disrupts priming[372]. And we have seen how *Plasmodium* infection and blood feeding leads to immune activation and granulocyte proliferation (which is mediated by HDF). However, it is not clear whether LL3 is essential for HDF synthesis or for hemocytes to respond to HDF. We found that LL3 is highly expressed in effector hemocytes and thus explored whether silencing LL3 affects the HDF response. Transfer of hemolymph from primed *A. gambiae* donors had HDF activity and elicited a strong priming response in control recipients injected with *lacZ* double stranded (ds) RNA, resulting in a prominent increase in circulating granulocytes, a modest increase in oenocytoids and a decrease in prohemocytes. This response was completely abolished when LL3 expression was silenced in the recipients by injection of dsLL3 RNA, indicating that LL3 and effector cells play a key role in orchestrating hemocyte responses to HDF [Fig. IV.4].

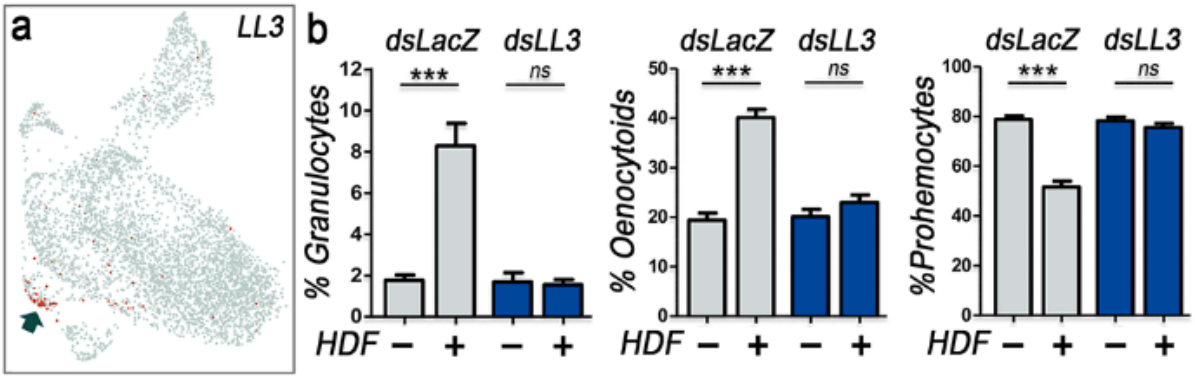

Fig. IV.4 LL3 is expressed in effector cells and required for hemocyte differentiation. (A) UMAP visualisation of all hemocytes by *LL3* expression. Red indicates cells with more than 1 UMI **(B)** Percentage of circulating granulocytes, oenocytoids and prohemocytes of *LL3*-silenced mosquitoes injected (+) or not (-) with HDF versus double-stranded *lacZ* RNA injected mosquitoes used as negative controls (**** P<0.0001, Unpaired t-test). Data are representative of two independent experiments (mean ± SEM).

3.3 Gene changes with blood-feeding and malaria infection

3.3.1 scRNA-seq

After looking at absolute changes in cell numbers we further probed the impact of *Plasmodium* infection on mosquito hemocytes by performing differential expression analysis on our scRNA-seq dataset with the Seurat Wilcoxon DE test as well as the Seurat implementation of MAST (see methods). As the MAST package produced similar numbers of significantly downregulated and upregulated genes when compared to the Wilcoxon-Rank Sum Test, we decided to use MAST for all DE analyses. The lists of positively regulated genes did not change by using MAST or Wilcoxon. Interestingly, when cells from day 7 post-infection were removed we found a heightened number of DE genes, suggesting *Plasmodium* largely modulates the immune system in the first three days of infection. However, prohemocytes saw the pattern reverse, with a higher DE gene count when including *P. berghei* day 7 prohemocytes in the analysis. Ooenocytoids did not seem to respond strongly to *P. berghei* infection at any time [Table IV.1]. Effector and secretory cells were too rare. Most DE genes were due to the activation of granulocytes, in agreement with the trajectory and differentiation analyses of the previous chapter. Genes upregulated included PPO2, 3, 4, 5, laminins, collagens and actins, CLIPB8, Tctp, Matuselah receptor 6, PGRPLD, LRIM6, Calreticulin, Cecropin 1, SCRC1. Downregulated genes included CLIPD1, fibrinogen, and fibronectins [Fig. IV5A].

Cluster	**DE genes – All days**	**DE genes - Day 1-3**
Fat Body	**75 (U:33-D: 42)**	**95 (U:45-D:50)**
Prohemocytes	**132(69-63)**	**10 (1-9)**
Granulocytes	**53 (23-30)**	**232 (119-113)**
All hemocytes w/o oenocytoids	**89 (39-50)**	**168 (108-60)**
All cells	**76 (36-40)**	**174 (99-75)**
Oenocytoids	**16 (2-14)**	**17 (16-1)**
Dividing cells	**1 (0-1)**	**3 (1-2)**

Table. IV.1. Summary of scRNA-seq *P. berghei* DE analyses. MAST package, filtered for absolute log fold change > 0.25 and Q-value <0.1. U = upregulated. D = downregulated.

Whereas granulocytes had 232 DE genes, of which 119 upregulated and 113 downregulated (days 1, 2, and 3 post *Plasmodium* infection), prohemocytes only had 10, of which 9 downregulated. However, when considering all time points the number of DE genes in prohemocytes was 132, of which 69 upregulated and 63 downregulated [Fig. IV.5B]. Many of the upregulated genes were shared between granulocytes and prohemocytes, including calreticulin, SPARC, Tctp, but there were some markers more specific to prohemocytes, including 14-3-3 protein epsilon, cofilin, FK506-binding protein 14, calmodulin, cellular nucleic acid binding protein, ARP, and PPO6.

Conversely, very few genes were differentially expressed in oenocytoids, including SPARC, and almost none in dividing cells and effector cells. Secretory cell had 26 upregulated genes during *P. berghei* infection. Top genes included all-*trans*- and 9-*cis*, SPARC, cathepsin F, ARP 2/3 complex, AKT, and PPO6. Fat body cells had 95 DE, of which 45 upregulated and 50 downregulated. Most downregulated genes in the fat body were not annotated, but among the few that were we could find phenoloxidase inhibitor protein, cathepsin L, autophagy related gene, or gelsolin, again indicating an increase in the immune activity of this organ.

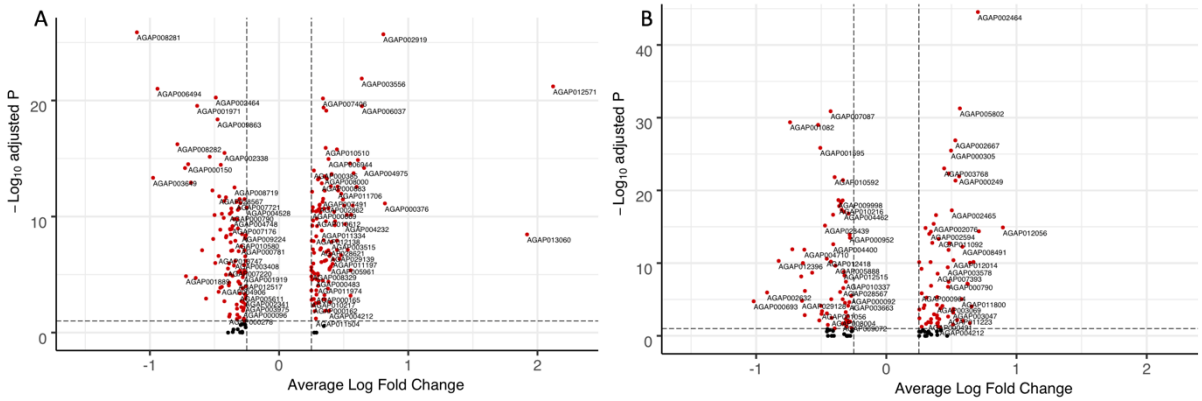

Figure IV.5 scRNA-seq DE gene analyses (A) Volcano plot of DE genes, granulocytes, day 1-3. (B) Volcano plot of DE genes, prohemocytes, days 1-7. DE with MAST package adapted for Seurat scRNA-seq pipeline. Filtered for absolute log fold change > 0.25 and Q-value <0.1.

3.3.2 Bulk RNA-seq

In parallel we performed the same analysis in our bulk RNAseq dataset, which had the same experimental design as the scRNA-seq experiments. In bulk hemocyte samples 65 genes were differentially upregulated (P-adjusted < 0.05 and Log_2 Fold >1) after *P. berghei* infection (day 1,2,3, and 7), including many immune effectors such as TEP1, APL1C, PGRPS3, PGRPS2, PGRPLB, PPO Inhibitor protein, CLIPs, SRPNs, and CTLs [Fig. IV.6].

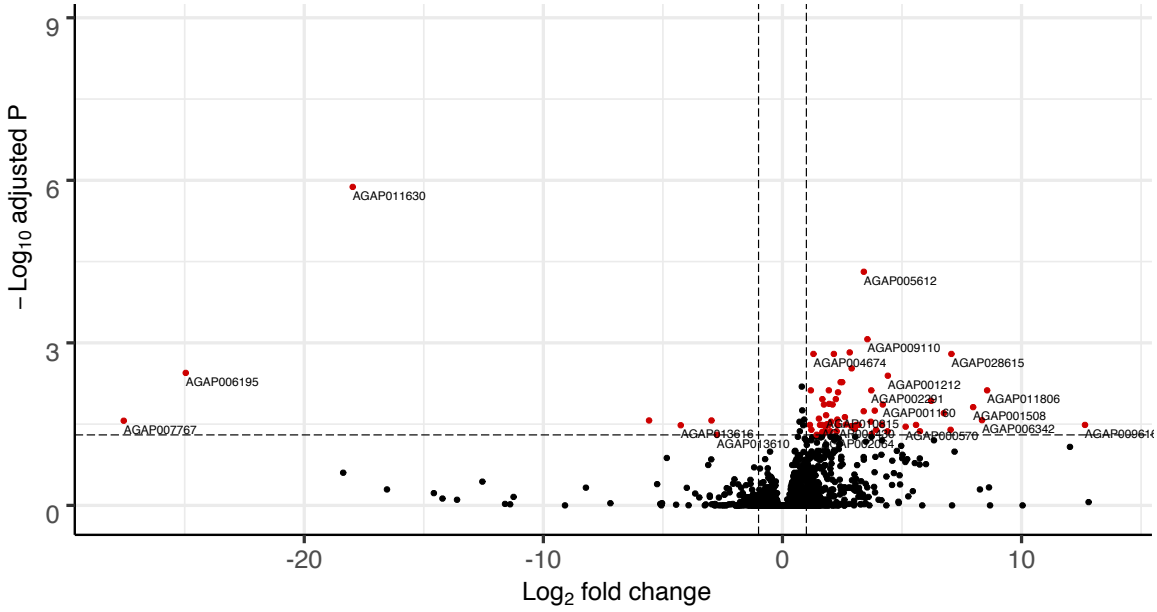

Fig. IV.6 Differential expression of *Anopheles* hemocytes – *P. berghei* vs blood-feeding. From a total of 12184 filtered genes, DE and upregulated genes during *Plasmodium* infection to the right, filtered for log2 fold change >1 and Q-value <0.05

Similarly, gut samples showed 502 upregulated genes during *P. berghei* infection, including a multitude of immune-related genes such as REL2 (IMD pathway signalling NF-kappaB Relish-like transcription factor), AGAP005933 (NFkappaB essential modulator), SCRC1, C-type lectins, APL1C, IAP2, PGRPLB, CLIPs, LRIMs, LL2 and LL3, TEP1, TEP4, TEP6, TEP14, Serpins, TRAF6 (TOLL pathway signalling TNF Receptor-Associated Factor), LYSC4, a PPO Inhibitor, and a Toll-interacting protein. TOLL1A, Ftz and Frizzled transcription factors, and DUOX were instead downregulated with infection [Fig. IV.7].

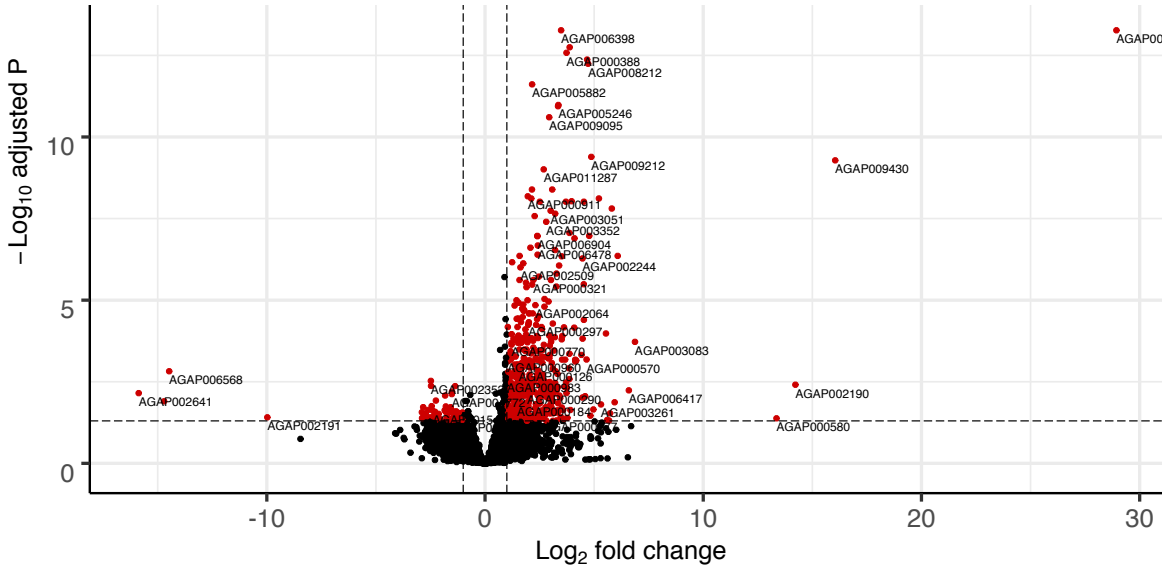

Fig. IV.7 Differential expression of *Anopheles* guts – *P. berghei* vs blood-feeding. From a total of 12726 filtered genes, DE and upregulated genes during *Plasmodium* infection to the right, filtered for log2 fold change >1 and Q-value <0.05

And finally, there were 10 upregulated genes and 10 downregulated genes in mosquito carcasses (fat body, ovaries, muscle, brain, skeleton, etc.) in response to *P. berghei* infection, showing a more subdued response compared to guts or hemocytes. Many DE genes are uncharacterized, but interestingly TRAF6 was upregulated in guts and carcasses [Fig. IV.8].

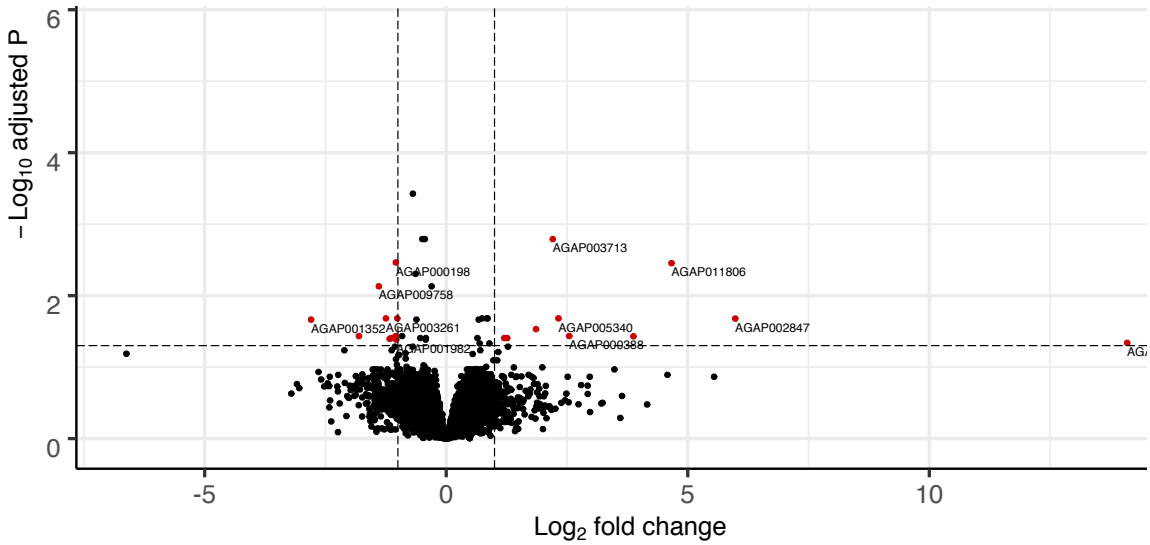

Fig. IV.8 Differential expression of *Anopheles* carcasses – *P. berghei* vs blood-feeding. From a total of 12952 filtered genes, DE and upregulated genes during *Plasmodium* infection to the right, filtered for log2 fold change >1 and Q-value <0.05

Conversely, blood feeding caused a tremendous rearrangement of the mosquito metabolism and transcriptional programming, in all tissues analyzed. When combining all samples together and performing a unified analysis 1731 genes were differentially expressed. Results were very similar when analyzing samples separately: 1778 DE genes if only looking at hemocytes, 1733 DE genes when analyzing the gut, and finally 1601 DE genes in the mosquito carcasses [Fig. IV.9]. A GO enrichment analysis showed that genes upregulated in sugar-fed conditions were involved in carbohydrate metabolism and transport. Conversely, mosquito carcasses were characterized by genes that involved in cellular reproduction, purine metabolism, DNA elongation and replication, lipid metabolism and transport (e.g. Vitellogenin). Many anti-microbial peptides and immune genes were also upregulated, such as defensins, gambicin, prophenoloxidases, Toll 1A, TNF receptor-associated factor 4, LRR [Fig. IV.10-11].

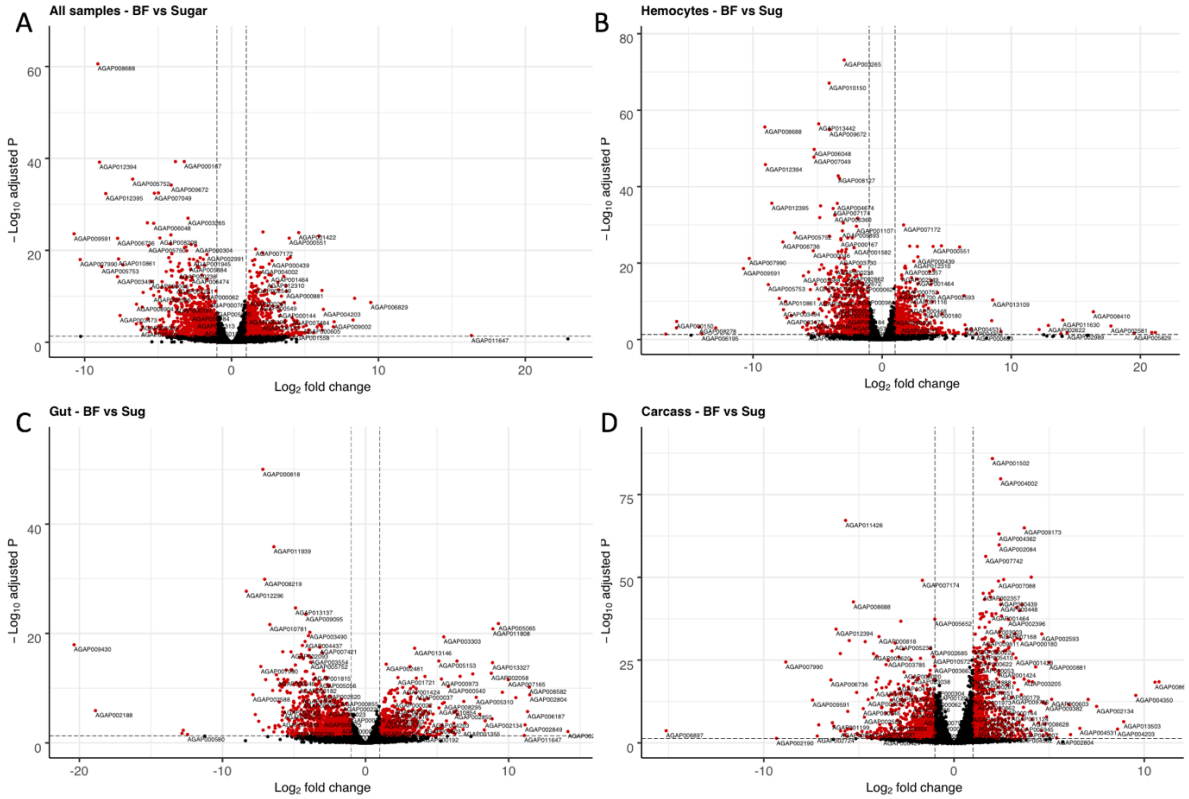

Fig. IV.9 Differential expression of *Anopheles* tissues – Blood feeding vs sugar feeding. From a total of 13048 filtered genes, DE and upregulated genes during *Plasmodium* infection to the right, filtered for log2 fold change >1 and Q-value <0.05 (A) All tissues combined (B) Hemocyte samples only (C) Gut samples only (D) Carcasses samples only.

GO:BP		stats	
Term name	Term ID	p_{adj}	$-\log_{10}(p_{adj})$ 0 ≤16
carbohydrate transmembrane transport	GO:0034219	3.861×10^{-5}	
hexose transmembrane transport	GO:0008645	4.724×10^{-4}	
monosaccharide transmembrane transport	GO:0015749	4.724×10^{-4}	
glucose import	GO:0046323	4.724×10^{-4}	
glucose transmembrane transport	GO:1904659	4.724×10^{-4}	
carbohydrate transport	GO:0008643	5.897×10^{-4}	
oxidation-reduction process	GO:0055114	6.750×10^{-3}	
xanthine catabolic process	GO:0009115	1.784×10^{-2}	
xanthine metabolic process	GO:0046110	1.784×10^{-2}	

Fig. IV.10 GO Enrichment – Sugar samples. From a total of 13048 filtered genes, DE and upregulated genes during *Plasmodium* infection to the right, filtered for log2 fold change >2 and Q-value <0.05, imported into G:Profiler as of methods section.

GO:BP		stats	
Term name	Term ID	p_{adj}	$-\log_{10}(p_{adj})$ 0 ≤16
'de novo' IMP biosynthetic process	GO:0006189	1.619×10^{-5}	
IMP biosynthetic process	GO:0006188	9.468×10^{-5}	
IMP metabolic process	GO:0046040	3.230×10^{-4}	
alpha-amino acid metabolic process	GO:1901605	1.144×10^{-3}	
small molecule metabolic process	GO:0044281	3.386×10^{-3}	
alpha-amino acid catabolic process	GO:1901606	4.774×10^{-3}	
purine nucleoside monophosphate biosynthetic process	GO:0009127	6.411×10^{-3}	
purine ribonucleoside monophosphate biosynthetic pro...	GO:0009168	6.411×10^{-3}	
DNA strand elongation involved in DNA replication	GO:0006271	7.805×10^{-3}	
DNA strand elongation	GO:0022616	7.805×10^{-3}	
DNA replication	GO:0006260	1.102×10^{-2}	
cellular amino acid catabolic process	GO:0009063	1.410×10^{-2}	
purine nucleoside monophosphate metabolic process	GO:0009126	1.697×10^{-2}	
purine ribonucleoside monophosphate metabolic process	GO:0009167	1.697×10^{-2}	
leading strand elongation	GO:0006272	1.762×10^{-2}	
lipid transport	GO:0006869	1.769×10^{-2}	
lipid localization	GO:0010876	1.997×10^{-2}	
cellular amino acid metabolic process	GO:0006520	3.056×10^{-2}	
purine nucleobase biosynthetic process	GO:0009113	3.350×10^{-2}	

Fig. IV.11 GO Enrichment – Fat body samples. From a total of 13048 filtered genes, DE and upregulated genes during *Plasmodium* infection to the right, filtered for log2 fold change >2 and Q-value <0.05, imported into G:Profiler as of methods section.

3.4 *P. berghei* infection increases FBN-7+ circulating hemocytes

We then further probed the changes brought about by *P. berghei* infection in circulating hemocytes by collecting cells from infected and blood-fed mosquitoes, and doing RNA-FISH with the markers described for each cell type in Chapter III. We quantified the expression of key RNA-FISH markers in over 3200 hemocytes (two biological repeats), and found an increase in the number of cells positive for fibrinogen (FBN7) after *P. berghei* infection, as compared to blood feeding. This was true both for LRR8+ hemocytes, where FBN+ cells went from 18% to 77% [Fig. IV.12], and PPO4+ oenocytoids, where FBN+ cells increased from 22% to 66% [Fig. IV.13]. While FBN7 was originally chosen as the RNA-FISH marker for secretory cells, the expression seems to be upregulated in all morphological cell types upon infection [Fig. IV 12-13]. There were no changes in the other markers.

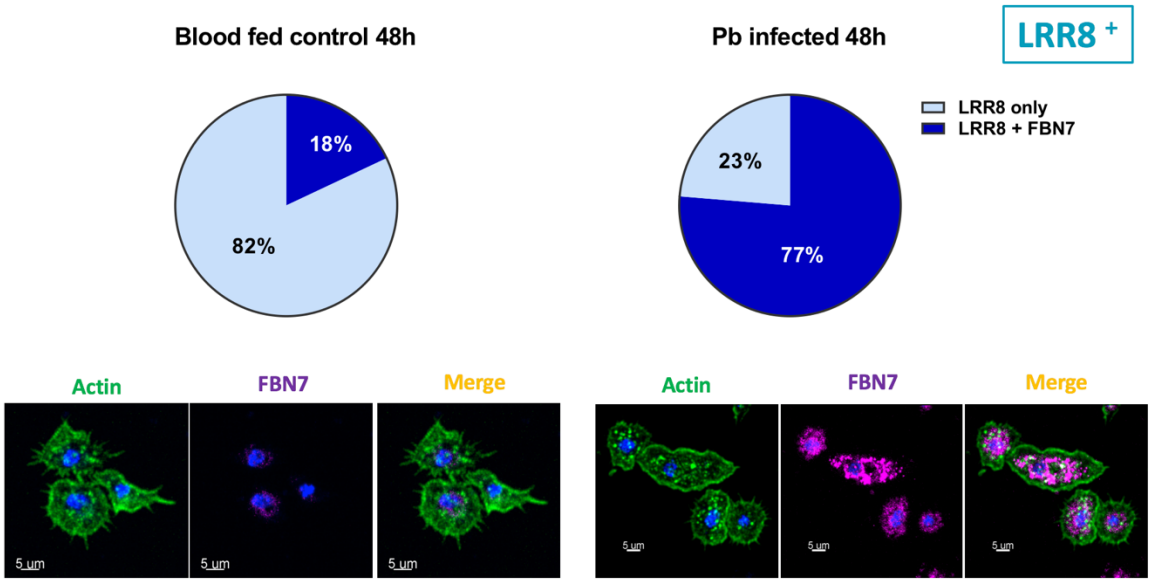

Fig. IV.12 *P. berghei* infection increases the number of FBN7+ hemocytes in circulation. From 3200 hemocytes, 2 biological repeats. LRR+ cells were considered.

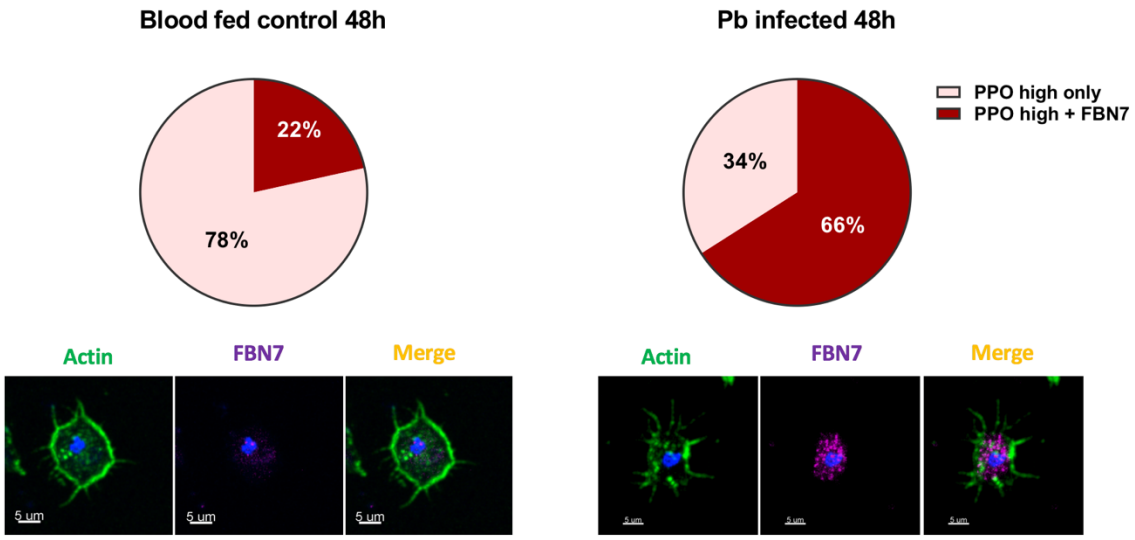

Fig. IV.13 *P. berghei* infection increases the number of FBN7+ oenocytoids in circulation. From 3200 hemocytes, 2 biological repeats. PPO4+ cells were considered.

3.5 *Plasmodium* recruits hemocytes from the fat body wall

Next, to understand how *Plasmodium* infection affects not only circulating but also sessile hemocytes (the hemocytes that are associated with mosquito organs and tissues) we did RNA-FISH on fat body walls and guts of blood-fed or *P. berghei* infected *A. gambiae* mosquitoes. There was a striking reduction in hemocytes per mm^2 of body wall (LRR8+ cells) in infected samples, from 286±76 to 90±34 /mm^2. Fibrinogen-CT+ (Secretory) and Transmembrane+ (Effector) cells remained constant: 6.7±6.1 vs 6.1±3.5 /mm^2 and 4.7±1.5 to 3.3±1.2 /mm^2 respectively. Oenocytoids were unchanged, 14.5±9.0 to 7.0±5.5 /mm^2, while total cells decreased from 312±85 to 106±41 /mm^2, largely due to LRR8+ cells [Fig. IV.14-15].

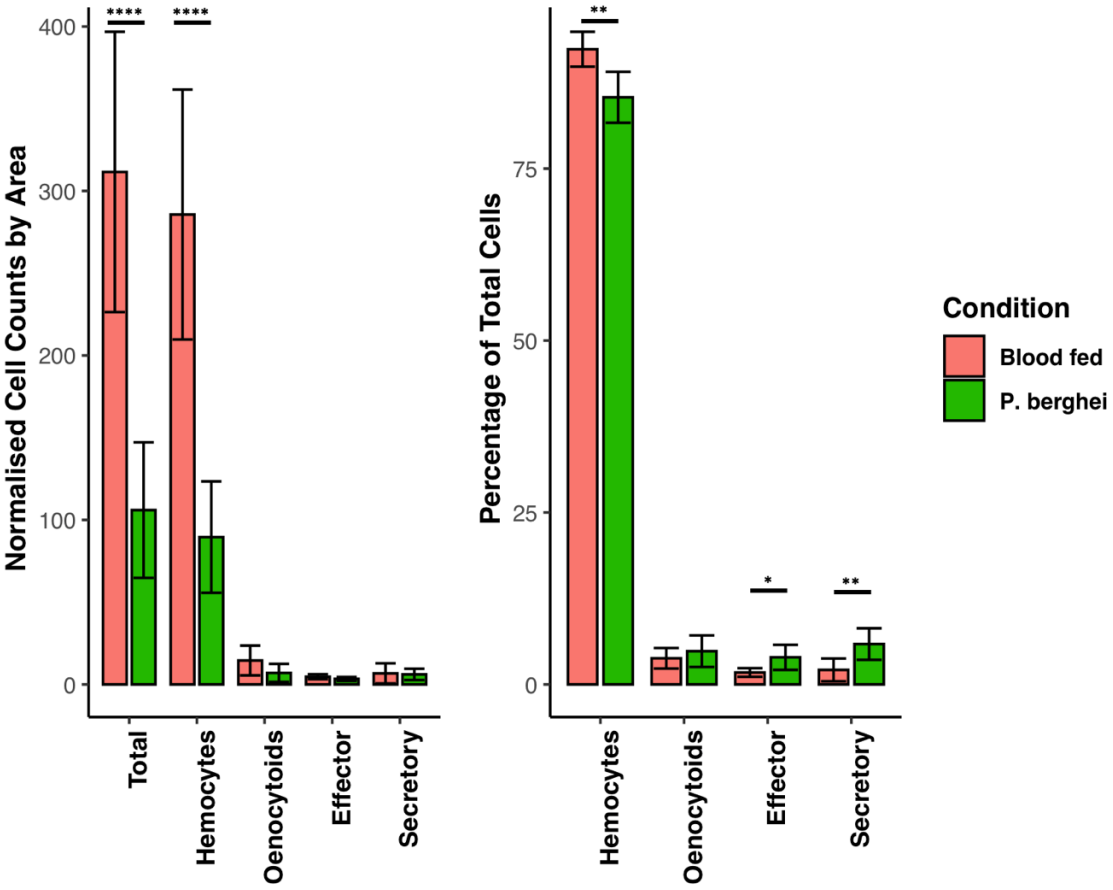

Fig. IV.14 Quantification of cell types on the body wall of *Anopheles* mosquitoes. 16 body walls of blood-fed and 12 of *P. berghei*-infected mosquitoes, followed by RNA-FISH. To the left cell counts normalized by mm^2 of body wall area. To the right percentages of each cell type from total RNA-FISH positive cells. Error bars indicate 95% Confidence Interval. **** ($P \leq 0.0001$), ** ($P \leq 0.01$), * ($P \leq 0.05$) – Welch T-Test. Three biological repeats.

Furthermore, while the percentage of LRR8+ cells also decreased from 92.4% (±2.5) to 85.4% (±3.7), and there was an increase in effector and secretory markers: from 1.7% (±0.6) to 3.9% (±1.8) and from 2.1% (±1.7) to 5.9% (±2.3) respectively, indicating recruitment of circulating hemocytes with infection. The percentage of oenocytoids instead remained unchanged, from to 3.8% (±1.5), to 4.8% (±2.3) [Fig. IV.14-15].

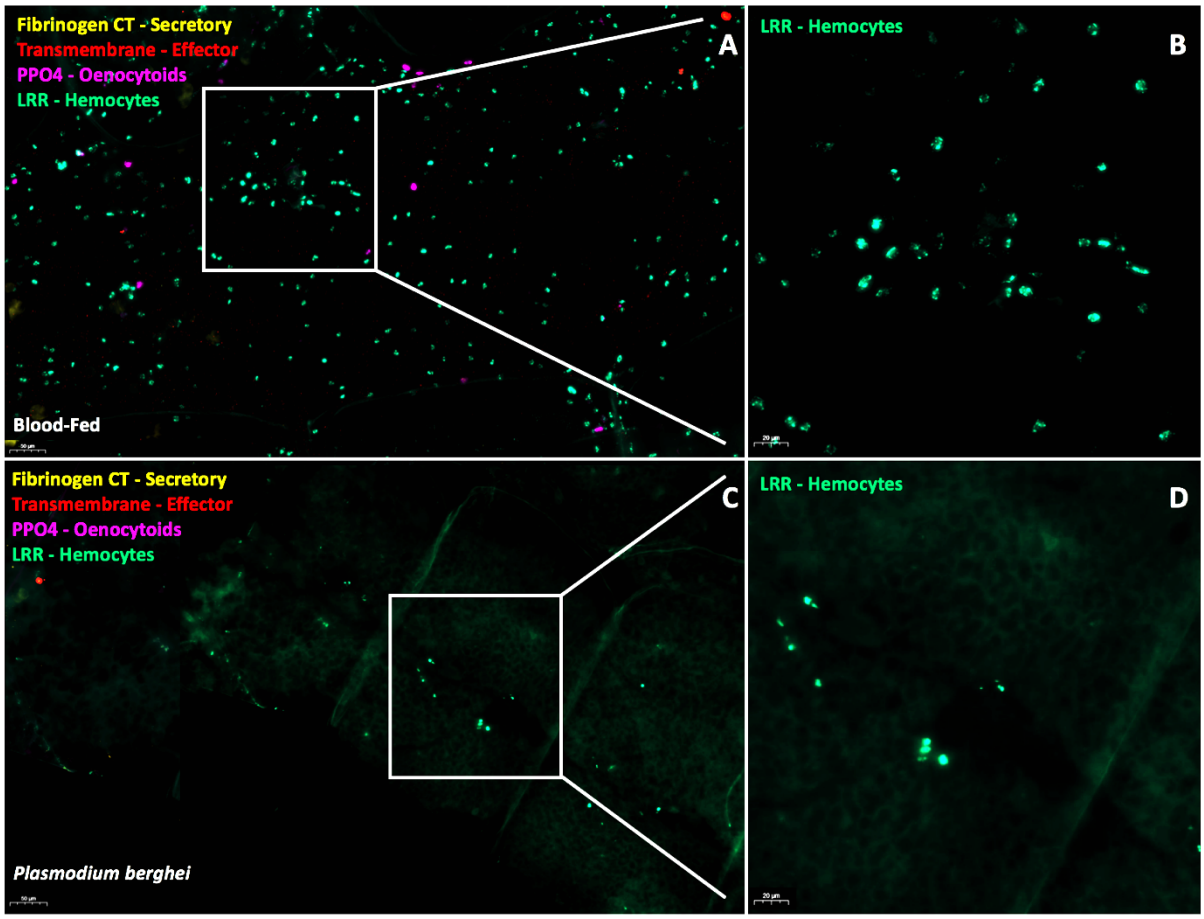

Fig. IV.15 Representative RNA-FISH image of *A. gambiae* mosquito body wall after infection. A total of 16 body walls of blood-fed *A. gambiae* and 12 of *A. gambiae* infected with *P. berghei* were processed following RNA-FISH protocol. (A-B) Blood-fed controls. (C-D) *P. berghei* infection (A, C) 20X magnification (B, D) 40X magnification.

Indeed, when we further explored the surface of the fat body of mosquitoes with electron microscopy we noticed granulocytes are only tenuously associated with the fat body, with immune cells only connected to the fat body by a few pseudopodia extending from the body wall. Our TEM experiment thus showed individual sessile hemocytes bathed by hemolymph and attached to the basal lamina of the tissues through pseudopods, indicative of a dynamic and potentially transient association, with granulocytes appearing ready to detach into circulation when responding to systemic stimuli such as *P. berghei* infection [Fig. IV 14-16].

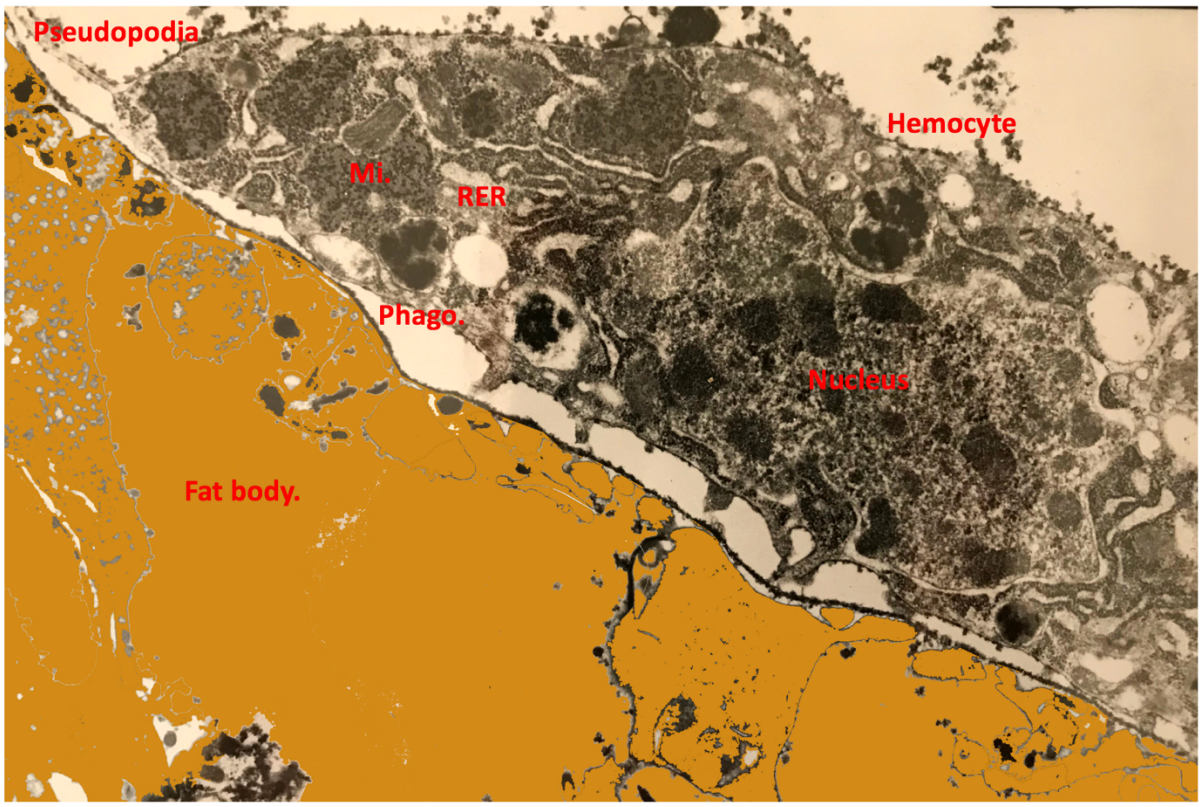

Fig. IV.16 Electron-microscopy image of granulocyte attached to fat body. Phago. = Phagosome. Mi. = Mitochondrion. RER = Rough Endoplasmic Reticulum. Fat body false-colored in yellow for orientation. Prepared by Rafael Cantera.

3.6 Effect of *P. berghei* infection to hemocyte numbers in the gut

More hemocytes per mm^2 were attached to the body wall than to the gut of *Anopheles* mosquitoes that were either blood-fed or infected with *P. berghei*, with a total of 23±6.6 vs 15±3.9 cells/mm^2. LRR8+ cells were also present in lower amounts, with 19.4±6.6 to 12.1±3.8 cells/mm^2, which was close to a statistically significant decrease (P = 0.053, Welch T-test). Normalised Fibrinogen-CT+ (Secretory), Transmembrane+ (Effector), and oenocytoids cell numbers were all unchanged: 0.38±0.26 to 0.13±0.12 cells/mm^2, 1.87±1.06 to 0.87±0.64 cells/mm^2, and 1.55±0.9 to 1.66±0.56 cells/mm^2 respectively. Percentages were all unchanged, but oenocytoids increased from 7.8% (±4.3) to 15.0% (±7.4), which was almost statistically significant (P=0.083 Welch T-test) [Fig. IV.17].

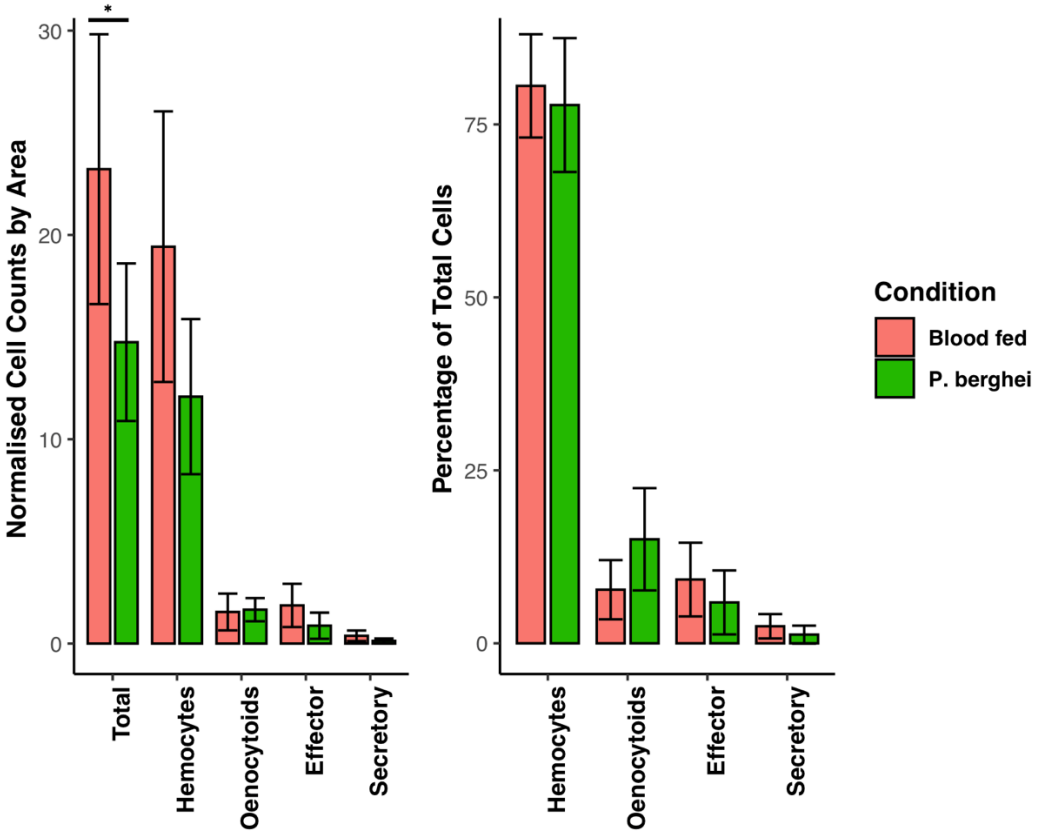

Fig. IV.17 Quantification of cell types on the gut of *Anopheles* mosquitoes. From 19 body walls of blood-fed mosquitoes and 17 of mosquitoes infected with *P. berghei*, followed by RNA-FISH as of methods. To the left cell counts normalized by mm^2 of body wall area. To the right percentages of each cell type from total RNA-FISH positive cells. Error bars indicate 95% Confidence Interval. * ($P \leq 0.05$) – Welch T-Test. Three biological repeats.

3.7 Effect of *P. falciparum* infection on sessile and motile hemocytes

To recapitulate our findings with a parasite more relevant to humans we repeated the experiments with *P. berghei,* but with *P. falciparum*. Similarly to *P. berghei* we found a trend towards decreased LRR8+ and total cell numbers attached to the body wall of mosquitoes with a Pfs47 knock-out *P. falciparum* which is unable to infect mosquitoes due to increase immune system clearance: 687 (±115) to 598 (±46) LRR8+ cells and 802 (±143) to 707 (±67) total cells per mm^2, albeit the decrease was not statistically significant (P = 0.145 and P = 0.128 respectively, Welch T-test). The trend seemed to be reversed by wild-type *P. falciparum* infection, with 712 (±152) LRR+ cells and 831 (±171) total cells per mm^2. All other normalized cell counts and percentages were the same except for an increase in oenocytoids, from 8.1% (±1.1) with blood-feeding to 10.9% (±3.1) with wild-type infection (P = 0.045, Welch T-test) and 10.5% (±2.2) with knock-out infection (P = 0.08, Welch T-test) [Fig. IV.18].

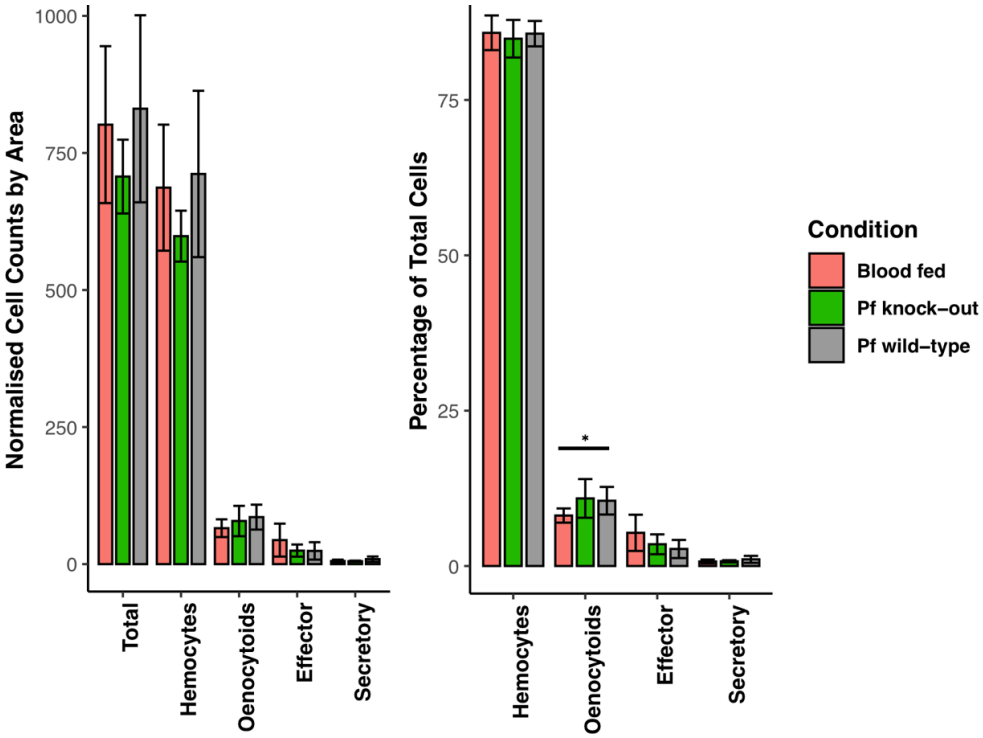

Fig. IV.18 RNA-FISH quantification of cell types on the body wall of *Anopheles*. From 6 blood-fed, 8 wild-type *P. falciparum*, and 8 Pfs47 KO *P. falciparum* mosquitoes. To the left cell counts normalized by mm^2 of body wall area. To the right % of cell type from total RNA-FISH positive cells. Error bars 95% CI. * ($P \leq 0.05$) – Welch T-Test. One biological repeat.

In the gut we again found a lower number of adherent hemocytes compared to carcasses. Cell numbers with blood-feeding were comparable: 23 (±6.6) in the *P. berghei* experiments and 34 (±20) in the *P. falciparum* experiments (per mm^2). The normalized counts showed no difference between *P. falciparum* infections and control, though confidence intervals were large due to low number of samples. We did find an increase in the percentage of LRR8+ cells (hemocytes) attached to the gut, which went from 52% (±19) with blood-feeding to 75% (±5.6) with wild-type infection (P = 0.013, Student T-test) and 69% (±11.5) with knock-out infection (P = 0.073, Welch T-test). At the same time, Transmembrane+ (Effector) cells decreased from 19.9% (±6.4) with blood-feeding to 7.3% (±5.4) with wild-type infection (P = 0.003, Student T-test) and 10.9% (±9.8) with Pfs47 knock-out infection (P = 0.060, Welch T-test) [Fig. IV.19].

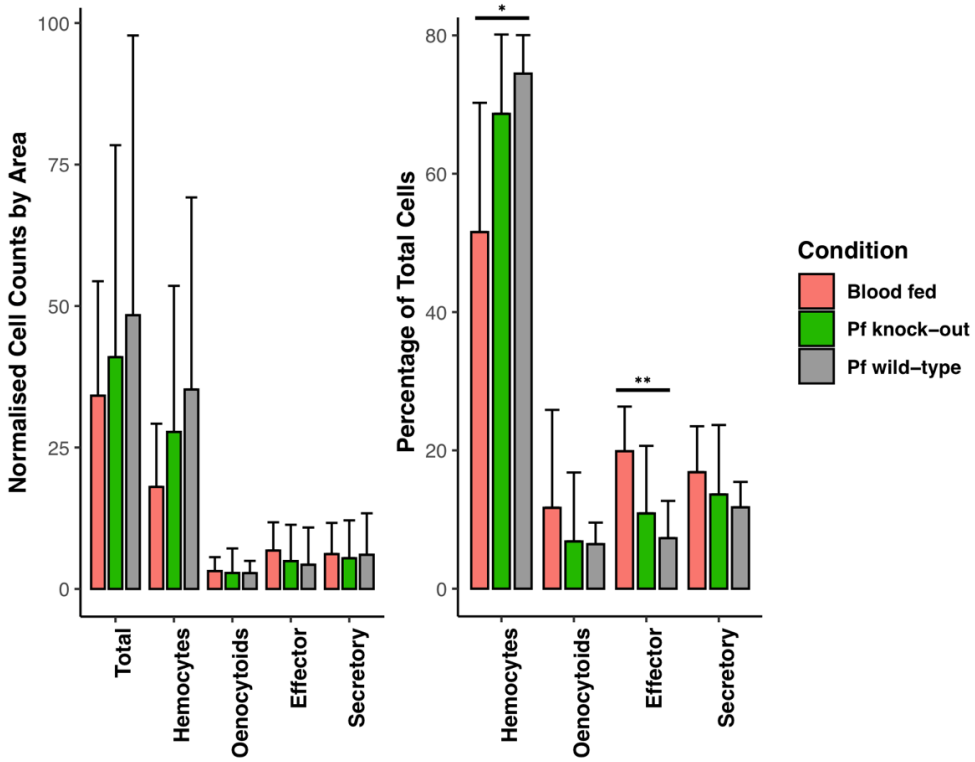

Fig. IV.19 RNA-FISH quantification of cell types on the gut of *Anopheles* mosquitoes. From 6 blood-fed, 6 wild-type *P. falciparum*, and 4 Pfs47 KO *P. falciparum* mosquitoes. To the left cell counts normalized by mm^2 of body wall area. To the right percentages of each cell type from total RNA-FISH positive cells. Error bars indicate 95% Confidence Interval. ** ($P \leq 0.01$), * ($P \leq 0.05$) – Welch T-Test. One biological repeat.

In order to recapitulate our findings with respect to the increase in FBN7 hemocytes after *P. berghei* infection we also looked at how FBN7+ hemocytes changed in circulation after *P. falciparum* infection. Again, we found that infection with the wild type *P. falciparum* significantly increased ($P < 0.0001$, Welch T-test) expression of FBN7 in hemocytes. Interestingly, the increase is abrogated by Pfs47 knock-out *P. falciparum* ($P = 0.02$, Welch T-test). FBN7+ cells went from 48.3% (±9.4) with blood-feeding to 83.6% (±11.3) with wild-type infection and 59.8% (±21.8) with knock-out infection. No other changes were observed [Fig. IV.20].

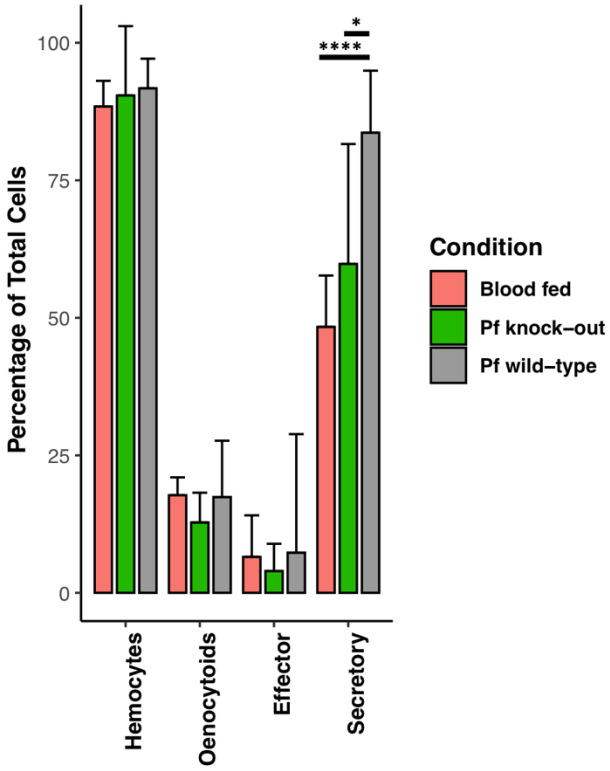

Fig. IV.20 Quantification of *Anopheles* hemocytes. From a total of 1066 blood-fed cells, 966 wild-type *P. falciparum* cells, and 1694 of Pfs47 knock-out cells (8 mosquitoes per repeat), followed by RNA-FISH as of methods. Error bars, 95% Confidence Interval. **** ($P \leq 0.0001$), * ($P \leq 0.05$) – Welch T-Test. Two biological repeat, two technical repeats each.

4 Discussion

In this chapter we looked at how the *A. gambiae* immune system responds to *Plasmodium* infection. First, we quantified the hemocyte cell clusters obtained via scRNA-seq in control (sugar-fed), and challenged conditions (blood feeding and infection). Both caused a decrease in the proportion of cells identified as prohemocytes. The proportion of inactive, baseline granulocytes was the same in sugar-fed and blood-fed mosquitoes, whereas infection caused a large increase in the number of active granulocytes (both type 1 and 2). This suggests a recruitment of baseline granulocytes to more active granulocytes states. Other terminal cells such as effector cells, oenocytoids, and rapidly dividing cells increased by the same amount with both blood-feeding and infection. Secretory cells are an exception and were mostly detected in blood-fed samples. Either secretory cells are up-regulated with blood feeding as a way to pre-empt invasions of bacteria, or our result was a spurious technical artefact due to mosquito manipulation. These are rare cells, and muscle cells were also detected more in blood-fed samples. It is possible secretory cells could be associated with wing muscles or cardio-vascular tissues. Fat body cells also increased with *P. berghei* infection. We hypothesize the increase is due to mosquito-wide immune responses causing cells to dislodge more easily. However, mobile fat body cells have recently been hypothesized to be genuine cells in circulation in the mosquito hemolymph. Indeed, at least some of the large number of fat droplets we observed via FACS in the mosquito hemolymph (Chapter II) could have been cells. If so, these cells could represent true, yet completely unexplored biology that will need to be investigated further.

We confirmed the number of hemocytes estimated by scRNA-seq with manual hemocyte counts, and they are reassuringly consistent. When the mosquito immune system is not activated, granulocytes are rare, whereas with activation (blood feeding and especially *Plasmodium* infection) large granulocytes can increase to double-digit percentages. We already described how prohemocytes and granulocytes lie in a continuum of transcriptomic similarity, as likely alternative cell stages along the same cell developmental trajectory. The relative absence of activated type 1 and type 2 granulocytes, effector cells, and dividing cells under

baseline conditions, and their increase with infection indicate these cells are what we identify as granulocytes via manual morphological microscopic analyses. Indeed, correlative microscopy experiments confirmed it. The only discrepancy between scRNA-seq and microscopy hemocyte numbers was for oenocytoids (~10% in the scRNA-seq dataset vs ~20% with microscopy quantification). Either these cells are more difficult to isolate and sequence, or not all cells that we previously morphologically identified as oenocytoids are in fact so. Correlative microscopy showed similarities between mature oenocytoids and maturing granulocytes, suggesting at least a partial overlap between these cell types, making manual morphological quantification more challenging.

Importantly, we discovered that the transcription factor LL3 is both highly and specifically expressed in a subset of hemocytes, the effector granulocytes. It had been separately shown that LL3 is expressed in hemocytes, and that silencing LL3 disrupt the mosquito's priming response[372]. However, the precise role of LL3 is priming was not clear. We found that systemically silencing LL3 abrogates the ability of mosquitoes to respond to an immune challenge, and that granulocyte numbers don't increase. Our results suggest that LL3, and the effector cells that express it, play an important role in coordinating hemocytes. However, we were not able to specifically target effector cells with our silencing because no appropriate experimental system existed. Our research will however provide the scientific community with the knowledge required to synthesise antibodies to specific hemocyte cell types. We hope future adoptive transfer experiments will fully elucidate the role of LL3 and effector cells in mosquito immune memory.

We then explored how *P. berghei* infection changes the transcriptomic landscape of mosquitoes. We performed DE analyses on both of our bulk and scRNA-seq datasets. In both, a large number of transcripts were differentially regulated in hemocytes in response to malaria infection. The effects of malaria infection peaked between one- and three-days post-infection, especially for granulocytes. When hemocytes obtained seven days post-infection were included in DE analyses the number of differentially expressed genes decreased, except for prohemocytes. Granulocytes thus appear to be the first cell type to respond, and prohemocytes

the last, consistently with the hypothesis that prohemocytes identified transcriptomically via scRNA-seq can include both morphological prohemocytes as well as some inactivated granulocytes.

There were many transcripts of interest upregulated in hemocytes upon infection. PGRPLD for example has been shown to increase *Plasmodium* infection prevalence upon knock-down [374]. CLIPB8 is required for prophenoloxidase activation and melanization of invading pathogens, and is highly upregulated by *P. berghei* infection [375]. Translationally-controlled tumor protein homolog (TCTP) has been shown to be an opsonin in silkworm and other hemocytes but has never before been implicated in the response against malaria, and could be a novel anti-plasmodial effector molecule [376]. The matuselah receptor 6 was also upregulated. A paralogue in *Drosophila* has been linked with effective immune responses and increased longevity [377]. Protein homolog 5 was upregulated with infection and has epigenetic functions. Memory in mosquitoes has long been thought to be mediated by epigenetic changes, and Cbx5 could be involved. Interestingly, an FK506-binding protein was also upregulated, especially in prohemocytes. This transcript is an orthologue of *Drosophila* FKBP39, is expressed throughout the life of *Drosophila* flies, binds DNA, is localized mostly in the nucleus, and could be a novel transcription factor important in immunity against *Plasmodium* [378]. In addition, calreticulin was also upregulated. Calreticulin has been shown to mediate phagocytosis and encapsulation in *Anopheles* mosquitoes as well as *Drosophila* [379, 380]. Another interesting transcript is the transcription factor BTF homologue 4, called "bicaudal" in *Drosophila*. During development bicaudal mutations have been shown to abort the establishment of the head. In addition, no hemocytes develop in these mutants. BTF4 could be important for hemocyte replication and development also in *Anopheles* mosquitoes [381]. Finally, GTP-binding nuclear protein Ran is an orthologue of *Drosophila* Ran, and is also involved in mitosis and cell division. In shrimp hemocytes it instead regulates phagocytosis, and in our dataset Ran was particularly upregulated in prohemocytes.

Most transcripts differentially expressed with infection in prohemocytes were also upregulated in granulocytes, but there were some interesting transcripts unique to

prohemocytes. For example, 'cellular nucleic acid binding protein' is an orthologue of a human protein that is involved in steroid signalling and proliferation. 14-3-3 protein epsilon is highly conserved in vertebrates and has been shown in lower organisms to promote anti-microbial hemocyte function. In addition, cofilin is involved in actin reorganisation and together with the actin-related protein (ARP) complex have important roles in immune responses and cytokinesis. Furthermore, granulocytes upregulated PPO2, 3, 4 and 5, while prohemocytes upregulated PPO6. And lastly, FK506-binding protein 14 expression in *Drosophila* has been shown to be activate Notch signalling and control lineage specification towards crystal cells (equivalent to oenocytoids) [382]. Whether late prohemocyte activation leads to oenocytoids differentiation remains an open question.

Interestingly, oenocytoids did not appear to strongly respond to infection. There were only ~16-17 DE transcripts, and no significant changes in the number of oenocytoids. Although the frequency of FBN7+ oenocytoids increased just as much as that FBN7+ granulocytes all in all our data suggests oenocytoids are not crucial mediators of anti-plasmodial defenses. On the other hand, fat body cells did respond, especially in the first few days (up to day 3) after infection. However, many up and downregulated genes in the fat body are not annotated, and much work remains to be done to elucidate what these genes do. Among annotated genes we saw downregulation of PPO inhibitor protein, LYSC4, and APG8, consistent with heightened immune activation. It has recently been proposed floating fat body cells may serve true immune functions, and in our hands the number of fat body cells did increase considerably after *P. berghei* infection. We hope future experiments will elucidate what these cells are and what function they possess in health and disease. Few genes were upregulated in dividing cells, effector cells, or secretory cells. However, secretory cells interestingly upregulated all-*trans*- and 9-*cis*-retinoic acids production. Both are important gene expression regulators and have essential roles in immunity, including cell proliferation and differentiation. Secretory cells could be releasing signals to activate nearby immune cells in response to infection. This hypothesis will also need to be tested in future experiments.

The immune response of *Anopheles gambiae* to malaria

Comparably fewer differentially expressed genes were detected with bulk RNAseq of hemocytes after *Plasmodium* infection, likely due to a dilution effect from a majority of non-responding cells. Among the genes that were upregulated we detected LL1 (LITAF-1) - a gene also upregulated in effector hemocytes and an LPS-responsive transcription factor - as well as TEP1, the key effector molecule for the early anti-*Plasmodium* responses. Furthermore, three peptidoglycan recognition proteins (PGRPs) were among the top differentially expressed genes. They are known immune regulators. PGRPS2 and PGRPS3 participate in antiparasitic defences, and PGRPLB was shown promote mosquito permissiveness to *P. falciparum* by deactivating the Imd pathway [374]. In addition, PPO inhibitor protein and CLIPA1 were upregulated. GO enrichment analyses found an enrichment of immune-related genes, confirming that hemocytes actively respond to malaria parasite infection.

In the gut on the other hand we found hundreds of upregulated genes during *P. berghei* infection, suggesting gut-intrinsic as well as hemocyte-mediated responses. Of all the tissues considered, the mosquito gut featured the highest number of DE genes. This is not surprising. *Plasmodium* ookinetes and oocysts mostly interact with the gut within the timeframe of our experiments. It would interest to confirm whether this is also true weeks after infection, as sporozoites move into salivary glands. The gut upregulated many important immune-related genes, including REL2/Imd. The REL2/Imd pathway is one of the two key nuclear factor-κB (NF-κB) immune pathways responsible for controlling *Plasmodium* infection, and the only pathway shown to mediate *P. falciparum* control, in addition to killing of viruses and Gram-negative bacteria [383]. Rel2 activation is mediated by transmembrane peptidoglycan recognition proteins (PGRPs). Then, the IKK-γ subunit of the IKK complex phosphorylates the Relish transcription factor, and IAP2 serves as an activator. IKK-γ, IAP2 and PGRPs were all upregulated in our hemocyte and gut samples with infection. We conclude that *P. berghei* activates the Rel2/Imd pathway in our mosquitoes. Rel1/Toll is the other key anti-plasmodial pathway, responsible for killing Gram-positive bacteria, fungi, and *P. berghei* [383]. Interestingly, 3 of the 4 most upregulated transcripts with infection were odorant binding proteins (OBP12, 38, 39), suggesting a role in immunity for this family of proteins. Ornithine decarboxylase was also highly upregulated both in the gut and in hemocytes. This protein is

thought to control macrophage activation and limit active macrophage M1 formation, suggesting hemocyte inhibition [384].

Unexpectedly, we could only detect 10 upregulated and 10 downregulated genes in mosquito carcasses, suggesting an absent or diluted immune response, and confirming the importance of using single cell rather than bulk approaches. We did nevertheless identify TRAF6 as an immune-related gene upregulated in the gut after infection. (TNFR)-associated factor 6 (TRAF6) is an adaptor protein first identified to mediate IL-1 receptor (IL-1R) NFκB activation. TRAF6 is now known to mediate TNFR, toll-like receptor (TLR), and tumor growth factor-β receptors (TGFβR) signaling to activate NFκB, MAPK, PI3K, and IRF, serving as a master regulator of immunity [385]. To our knowledge this is the first time TRAF6 has been involved in anti-plasmodial immunity.

Conversely, when we analysed the response of mosquitoes to blood feeding vis-à-vis sugar feeding we observed a complete rearrangement of the mosquito metabolism. Thousands of genes were differentially expressed, and our GO analysis showed the expected downregulation of sugar and xanthine metabolism and transport transcripts after blood-feeding (glucose, hexose, simple and complex sugar movement and catabolism), whereas transcripts involved in lipid metabolism and transport were upregulated. Blood-feeding turns the mosquito into a biosynthetic factory, upregulating transcripts involved in IMP and purine biosynthesis, amino acid metabolism, protein glycosylation, protein folding, and ER / membrane protein targeting. In addition, blood-feeding signals the start of the reproductive life-cycle of mosquitoes, with the production of fertile eggs. In our GO analyses the most significantly upregulated transcripts were indeed those involved in DNA replication initiation, DNA processing, (such as DNA geometric change and unwinding), DNA integrity checkpoints, mitotic checkpoints, and mitotic cell cycle.

We then explored the spatial dynamics of the *A. gambiae* immune response to *Plasmodium*. We leveraged RNA-FISH to observe how infection changed the proportion of sessile, tissue-resident hemocytes in the guts and carcasses of mosquitoes, and of motile

hemocytes in circulation. There were two major changes. First, hemocytes (likely granulocytes due to large cellular size and high LRR8 expression) were recruited in large numbers from the body wall of mosquitoes into the circulation. The marked increase in type 1 and type 2 granulocytes observed with infection would thus appear not to be solely caused by the heightened activation, replication, and differentiation of existing circulating hemocytes, but also by the recruitment of a reservoir of hemocytes attached to the body wall of mosquitoes. Indeed, when the interaction between hemocytes and fat body was probed in more detail by electron microscopy, we observed that the connection between these cells is tenuous at best, with hemocytes almost "walking" on the fat body, connected only through a few pseudopodia spreading from the central body of the cell, and thus readily dislodged. While the *P. falciparum* results are not conclusive due to the low number of samples, we observed a decreased number of LRR8+ cells attached to the midgut of mosquitoes infected with a *P. falciparum* Pfs47 knock-out line that is susceptible to immune killing by the mosquito immune system, whereas wild-type *P. falciparum* infection did not seem to change the number of attached hemocytes. Wild-type *P. falciparum* is able to masque its presence from the mosquito, and not activate immune responses, whereas *P. berghei* is not able to do so. Blocking hemocyte recruitment in the circulation could be one of the ways through which *P. falciparum* is able to survive in the mosquito.

The second main finding - a large increase in the number of hemocytes expressing fibrinogen (FBN7), a marker of secretory cells - was more surprising. Very few cells were positive for fibrinogen-CT (FBN7) in our scRNA-seq dataset. Conversely, the vast majority of motile hemocytes in circulation (upwards of 80%) becomes positive for FBN7 when mosquitoes are infected with *P. berghei*. The result holds true also for wild type *P. falciparum*. A Pfs47 *P. falciparum* knock-out, incapable of developing past the oocyte stage because of successful targeting and killing by the mosquito immune system, does not elicit the same response. Instead the number of FBN7+ cells is equal to that of blood feeding. More work will need to be done to fully understand the role of FBN7 and FBN7+ cells after *Plasmodium* infection. Other scRNA-seq markers of secretory cells included anti-microbial peptides,

Cathepsin L (perforin activator) - which in vertebrates promotes NK cell cytotoxicity - and Cathepsin F, which in invertebrates is involved in MHC II antigen presentation and Th1-immune responses [386]. An intriguing speculation is that the malaria parasite is able to skew the immune response towards an microbicidal state, akin to M2 state of macrophages in vertebrates, while at the same time blocking – and protecting itself from – the more potent phagocytic M1-like granulocyte activity. However, while Cathepsin-L is indeed downregulated in activated, IFN-γ treated, M1 human macrophages [387], these cells also upregulate ferritin, which is a conserved inflammatory response of activated M1 macrophages. Furthermore, secretory cells are also characterized by high levels of CLIPB4, important to control *P. berghei* infection. In addition, lineage tracing showed secretory and effector cells to be relatively similar. As such, it is also possible that fibrinogen-CT(FBN7) is instead upregulated as a general non-specific response to the gut wounds that are a result of *Plasmodium* ookinetes' midgut penetration, but that the expression is so low that our scRNA-seq library preparation was not able to capture it.

Finally, with RNA-FISH we saw a decrease in the number of effector hemocytes attached to the mosquito gut during *P. falciparum* WT infection. Infection with Pfs47 KO *P. falciparum* instead showed the number of effector cells to increase back to normal. If our hypothesis is correct and effector cells are modulating the immune system to respond to malaria infection then our results consistently suggest WT *P. falciparum* is able to blunt mosquito immune responses, and thus limit the number of anti-plasmodial effector cells. The identity of these cells will need to be explored further. These are large, rare cells, bigger than normal granulocytes, and could thus be the equivalent of *Drosophila*'s lamellocytes, which until now were not thought to exist in *Anopheles*.

Final summary & discussion

As we have seen, *Anopheline* mosquitoes are responsible for transmitting *Plasmodium* parasites to humans, and are the causative agent for over 219 million cases of malaria, and over 400,000 deaths annually[388]. However, the mosquito's immune system is far from being a passive bystander, and can limit *Plasmodium* infection in several ways[364, 365]. Hemocytes, the mosquito's equivalent of our white blood cells, are key players in these defensive responses, both through direct killing and through their role in complement activation and consequent parasite lysis. Infection with *Plasmodium* leads to a heightened state of immune activation in mosquitoes called priming. Primed mosquitoes are then able to mount a stronger immune response to subsequent infections. This response has been shown to be due to the release of a hemocyte differentiation factor (HDF) into the hemolymph[370], which is sufficient to increase the proportion of circulating granulocytes (the active subtype), as well as to promote hemocyte microvesicle release and subsequent complement activation[367].

When I started working on this project three hemocyte types, both circulating and sessile, had been described in *Anopheles gambiae* based on cellular morphology[389]. Granulocytes (10-20 μm) are the main phagocytic cells, while oenocytoids are smaller round cells 8-12 μm in diameter responsible for producing melanin, crucial for wound healing and pathogen encapsulation. And lastly, small round prohemocytes (4-6 μm) were thought of as the precursor cells of the other two cell subtypes. However, the full functional diversity of mosquito hemocytes was unexplored, their developmental trajectories were completely unknown, and it was unclear how much morphologically similar hemocytes are also functionally equivalent.

In this thesis I used single cell RNA sequencing (scRNA-seq) to profile the transcriptomes of 8506 hemocytes of *Anopheles gambiae* and *Aedes aegypti,* two important mosquito vectors. Blood feeding, infection with malaria parasites and other immune challenges revealed a previously unknown functional diversity of hemocytes, with different types of

granulocytes expressing distinct and evolutionarily conserved subsets of effector genes. A new cell type, which we term effector granulocytes, was defined in *Anopheles* by a unique transmembrane protein marker (TM7318) and high expression of LPS-Induced TNF-alpha transcription factor 3 (LL3). Knock-down experiments indicated that LL3 mediates hemocyte differentiation during immune priming. We identified two main hemocyte lineages and differentiation pathways in prohemocytes and granulocytes and found evidence of proliferating granulocyte populations. We discovered new hemocyte populations and markers of immune activation for each. We validated our analysis with RNA in-situ hybridization to integrate the transcriptional profiles with morphological analysis of circulating hemocytes and highlighted the mobilization of sessile hemocytes into circulation upon infection. And a comparison of *Anopheles* and *Aedes* hemocytes showed differences and similarities between these two mosquito species.

scRNA-seq revealed new types of hemocytes

First, circulating hemocytes were collected from adult *A. gambiae* M form (*A. coluzzii*) females that were either kept on a sugar meal or fed on a healthy or a *Plasmodium berghei*-infected mouse. Transcriptomes from 5,383 cells (collected 1, 3, and 7 days after feeding) revealed nine major cell clusters. Two clusters originated from adipose tissue and one from muscle tissue. Baseline fat body cells expressed several immune-modulatory genes such as CLIPs, LRIMs, lectins, and SRPNS, while active fat body cells expressed high levels of vitellogenin after blood feeding, a canonical marker of the mosquito fat body[390]. Based on their unique transcriptional profiles, we then identified six hemocyte clusters, including known cells such as oenocytoids, with high mRNAs levels of prophenoloxidases (e.g. PPO4 and PPO9), and granulocytes. We then selected hemocyte specific genes markers for our hemocyte lineages by combining scRNA-seq expression data with parallel bulk RNAseq data from different tissues. Oenocytoids contained low levels of leucine-repeat protein 8 (LRR8) mRNA, whereas granulocytes had an inverse pattern (low or absent PPO4 and high LLR8 levels).

In situ hybridization using these markers confirmed the oenocytoid-like round morphology (with few granules and pseudopodia) of circulating PPO4^{high}-LLR8^{low} cells, while PPO4^{low}-LLR8^{high} cells looked like prohemocytes and granulocytes (prominent pseudopodia and abundant granules). These two cell types appear to lie in a continuum of transcriptomic similarity, and while they shared many markers such as SPARC, cathepsin-L and LRR8, they differed in the amount of UMIs (73% fewer in prohemocytes). Dividing granulocytes were characterised by shared granulocyte markers, as well as their own unique subset of markers including cyclin B, aurora kinase and other mitotic markers. Secretory and effector hemocytes were both are negative for PPO4 and LLR8^{low}, but while effector hemocytes were large cells (25-40 μm) that expressed high levels of an uncharacterized transmembrane protein AGAP007318 (TM7318) and LPS-induced TNF-alpha transcription factor 3 (LL3), secretory hemocytes were smaller cells negative for both markers and instead expressing antimicrobial peptides such as defensin 1 and cecropins 1.

Mosquito hemocyte lineages in *Anopheles*

To investigate hemocyte differentiation dynamics, we then re-clustered the *Anopheles* cellular transcriptomes at higher resolution and performed lineage tree reconstruction with partition-based graph abstraction (PAGA) and found that proliferating cell were connected with the main granulocyte population which in turn was linked to effector cells and secretory antimicrobial granulocytes and prohemocytes. Sub-clusters within the major granulocyte populations reflected transcriptional responses to feeding and *Plasmodium* infection. Our findings were confirmed with both diffusion maps and slingshot analyses. They suggest the existence of a proliferative cell population that can replenish the pool of granulocytes, which can then differentiate further into more specialized regulatory or end-stage cells represented by effector and secretory cells without the need for further proliferation. Our data suggests that granulocyte proliferation and prohemocyte differentiation both appear to contribute to the observed increase in granulocyte numbers after blood feeding. However, the placement of prohemocytes in the granulocyte lineage tree should be considered tentative due to the few markers uniquely characterising prohemocytes. Prohemocytes are proposed to be precursors to both granulocytes and oenocytoids but the latter were transcriptionally disconnected from other

hemocyte subtypes, and we did not observe transcriptional markers of cell proliferation in oenocytoids. This suggests oenocytoids may represent a wholly separate lineage with origins either in larval stages or in other adult tissues. Alternatively, oenocytoids could derive from granulocytes, but due to a low differentiation rate we may not have captured intermediate cells.

To assess which of the newly discovered cell types are shared between anopheline and culicine mosquitoes, we also analysed the single-cell transcriptome of 3123 cells from *Ae. aegypti*, a vector for several relevant arboviruses including dengue. As with *Anopheles*, a dimensional reduction plot showed both canonical hemocytes and other cell types such as fat body cells and muscle cells. Our cross-species analysis revealed conserved transcriptome signatures for oenocytoids (99% and 77% correlation with *Anopheles* oenocytoids), and granulocyte subtypes, including antimicrobial cells (94% with secreting hemocytes), and proliferating granulocytes (87% with dividing granulocytes in *Anopheles*). Granulocytes and prohemocytes were again positioned on a continuum of transcriptomic similarity, with four different cell states, including a proliferating S-phase granulocyte cluster without a clear *Anopheles* equivalent. Granulocyte cells instead expressed laminins, leucine-rich repeat proteins, scavenger receptors, Toll receptor 5, and the transcription factor Rel2. Conversely, *Anopheles* effector granulocytes lack a counterpart in *Aedes*, and furthermore the main gene marker appear to be restricted to African and Asian *Anopheles*, suggesting effector hemocytes could be unique to a subgroup of *Anopheles* mosquitoes.

Transcription factor LL3 is required for hemocyte differentiation during priming

LL3 had been previously detected in granulocytes in response to *Plasmodium* infection. And LL3 silencing had been shown to abolish the *Anopheles* priming response[372]. Since we found LL3 to be a specific marker of effector granulocyte we explored whether silencing LL3 affects the ability of hemocytes to respond to HDF and we found the priming response to be completely abolished when LL3 expression was silenced in mosquitoes that had received HDF, suggesting LL3 and effector granulocytes play an important role in orchestrating the hemocyte priming response.

Blood-feeding and *Plasmodium* infection trigger granulocyte activation and mobilization

Finally, we explored how the cell types we described respond to malaria infection. It had been previously shown that the proportion of circulating granulocytes was low (1-3%) under normal conditions but increased after *Plasmodium* infection[370]. However, it was still unknown whether the increase was due to proliferation and differentiation of circulating progenitor cells, or mobilization of sessile hemocytes. Our transmission electron microscopy of individual sessile granulocytes attached to the basal lamina of the tissues through were indicative of a dynamic and potentially transient association. To explore that possibility, we used whole tissue mount *in situ* hybridization to find most sessile hemocytes to be $PPO4^{low}/LLR8^{high}$ granulocytes whereas oenocytoids, effector, and secretory cells are rare. Importantly, we found a dramatic reduction of sessile $PPO4^{low}/LLR8^{high}$ granulocytes in response to *Plasmodium* infection and no significant difference in the numbers of sessile oenocytoids, effector, or secretory cells.

Lastly, in circulating hemocytes both *P. berghei* and *P. falciparum* infection induced a significant increase in the proportion of FBN7 positive cells, indicating that this is a general marker of hemocyte immune activation. Combined, our results suggest that hemocyte recruitment from the body wall, granulocyte activation and proliferation, and prohemocyte differentiation can all contribute to boost circulating granulocyte numbers upon immune challenge.

Final considerations and outlook

Our knowledge of cellular immunity in vertebrates relies critically on understanding the functional diversity of cell types, their developmental trajectories and their trafficking dynamics. This thesis represents significant progress towards this understanding for two invertebrate immune systems that limit the vectorial capacity of mosquitoes for deadly human diseases such as malaria and Dengue. We confirmed the existence of oenocytoids and granulocytes and with gene markers we related cellular morphology to a more comprehensive molecular characterization of these cells. Unlike current thinking in the field we show

prohemocytes and granulocytes are closely related cells, and furthermore discovered the transcriptional profiles and molecular markers of novel hemocyte subtypes (effector, dividing, and secreting granulocytes), as well as fat body cells with immune-modulatory functions.

We defined two main hemocyte lineages in *A. gambiae*: the oenocytoid lineage, and the prohemocyte-granulocyte lineage. The latter can be further split into three sub lineages leading to differentiated effector, antimicrobial, or dividing granulocytes. We unearthed their precise molecular diversity and showed them to be largely conserved between distantly related mosquito genera and as such presumably of functional importance. However, we were not able to find effector granulocytes in *Aedes* mosquitoes. These cells have a unique, large morphology, and specifically express LL3. Silencing this transcription factor provided tentative evidence for a regulatory role of these cells in immune priming. However, we cannot rule out that other hemocyte types or mosquito tissues express LL3 and might thus be directly affected by LL3 silencing.

The cell-type markers and FISH probes we identified and validated will allow investigators to probe the immune functions of effector granulocytes and other specialized hemocyte types in detail. We leave open the question of the developmental origin of oenocytoids, but we identify two potential origins for the expansion of circulating granulocytes after immune challenge (blood feeding or *Plasmodium* infection). One is the mobilization of sessile granulocytes from the body wall, the other is a pool of proliferating, oligopotent granulocytes. Whether prohemocytes, which are transcriptionally related but less responsive than granulocytes, can transform into granulocytes and whether they can enter the cell cycle, also remains to be discovered.

In summary, the cell-type-specific marker genes, reference transcriptomes, and companion website (https://hemocytes.cellgeni.sanger.ac.uk/) from our study provide the first atlas of medically relevant invertebrate immune cells at single cell resolution and will serve as a resource for the field, providing a starting point for the type of lineage tracing and functional experiments which, in vertebrates, are resolving the developmental origins and functions of diverse immune cell populations.